JOTCS A

Journal of the Turkish Chemical Society
Section: A

Chemistry

An open access-based scholarly chemical journal

http://dergipark.ulakbim.gov.tr/jotcsa

Published, in English, in every August and February

Turkish translations of the titles and abstracts are available.

TURKISH
CHEMICAL SOCIETY

jotcsa@turchemsoc.org

Correspondance to:
Dr. Barbaros AKKURT, PhD, Managing Editor

Turkish Chemical Society
Halaskargazi Str. Uzay. Apt. No:15 D:8, Harbiye-Sisli-Istanbul/Turkey

e-ISSN: 2149-0120

JOTCS
Journal of the Turkish Chemical Society
Section: A
Chemistry
TURKISH CHEMICAL SOCIETY

Editorial Board, JOTCSA

(Sorted by the lastnames)

JOTCSA, volume 2, issue 4 (2015), pp. 1-11

Research Article

http://dergipark.ulakbim.gov.tr/jotcsa

Copper Octoate: A Commercially Available and Cost-Effective Homogeneous Catalyst for the Facile Synthesis of 2,2'-arylmethylenebis(3-hydroxy-5,5-dimethyl-2-cyclohexene-1-ones)

Rahim Hekmatshoar,*[1] Mojgan Kargar,[1] AbdolJalil Mostashari,[2] Zahra Hashemi,[1] Fereshteh Goli,[1] and Farnoush Mousavizadeh[1]

[1] Department of Chemistry, School of Science, Alzahra University, Vanak, Tehran, Iran.
[2] Industrial Chemical R&D Organization, Tehran, Iran.
*E-mail: rhekmatus@yahoo.com

Abstract: A practical and convenient approach for the synthesis of 2,2'-arylmethylenebis(3-hydroxy-5,5-dimethyl-2-cyclohexene-1-ones) was presented using copper octoate as a homogeneous catalyst. Copper octoate as an eco-friendly, low cost, and commercially available catalyst, reduced reaction times effectively to (16-50 min) while the reaction profiles were absolutely clean and no side products including dehydrated xanthene heterocycle were detected. Pure target compounds were obtained in very good to excellent yields (83-91%) via straightforward work-up procedure. The catalyst was recycled in the form of solution, up to four times, with no noticeable drop in activity.

Submitted: December 23, 2014. **Revised:** January 13, 2015. **Accepted:** February 13, 2015.

Keywords: Copper octoate, copper(II) 2-ethylhexanoate, homogeneous catalyst, arylmethylenebis(3-hydroxy-2-cyclohexene-1-one).

Introduction

Application of transition metals as catalysts in organic reactions has achieved widespread acceptance within the synthetic organic community. The gradual realization that complexes of transition metals have a place in synthetic procedures has caused a quiet revolution. Today, there are very rare complex total syntheses that do not involve at least a few transition metal-mediated reactions as key steps. In fact, highly reactive and normally unavailable reaction intermediates can be generated by applying transition metal complexes, and be used as reagents in organic synthesis. Performing some of the metal-catalyzed organic reactions in relatively large scales shows that the aforementioned methods are more than just academic interest [1, 2].

Copper(II) 2-ethylhexanoate ($Cu(EH)_2$), or copper octoate (Figure 1), is a well-known industrial reagent. It has been used as a preservative in wood industry for several years [3] and is also applied for the preparation of superconductors [4-6]. Because of its long-lasting effect in protection against termites and other insects, it is usually applied in bottom paints of ships. In addition, copper octoate is utilized as rot-proofing agent in textiles and may be applied on textile fabrics by dipping or spraying. Moreover, as a fungicide and bactericide, it has found various applications in household and agricultural products to control a considerable range of plant diseases. Copper octoate has also been used as a catalyst in many organic transformations such as polymerizations [7], preparation of allylic alcohols, and alpha, beta-unsaturated carbonyl compounds from the rearrangement of epoxides [8], aldol reaction [9],

oxidative coupling of indoles or pyrroles with enolates [10, 11] and oxidative coupling of esters or ketones with amides [12]. There is also a report of utilizing copper octoate as an ignition temperature-depressing agent which is applied as an additive to the fuel supply to promote oxidation of collected soot extracted from the exhaust gas of the engine [13]. An industrial example of using copper octoate as catalyst is its common application as a paint drier. Hydrocarbon chains help absorption of oxygen from the air and copper, on the other hand, acts as a catalyst to speed up the formation of the oxidative coating [14].

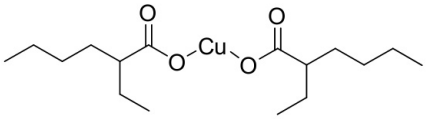

Figure 1. Copper octoate.

Copper octoate and many other metal complexes of 2-ethylhexanoic acid are often described as salts, while, indeed, they are not ionic but charge-neutral coordination complexes. The structure of copper octoate, both in crystalline [15] and solution [16] state, has been investigated. Low polarity and ionic character of copper octoate in addition to its long hydrocarbon chains are the major reasons for the high solubility of copper octoate in organic solvents like xylene and oils, which play a major role in finding extensive and novel applications both in industry and academia [17]. For instance, oxidative intramolecular cyclization of alkenyl amides was carried out successfully in the presence of copper octoate while its acetate salt did not perform well. It was mentioned as a reason that copper octoate has both the comparable activity with copper acetate and a high solubility in the reaction medium which causes homogeneity in the reaction medium [18]. Indeed, combining less toxicity and non-corrosive nature of solid acids and the motility of liquid acids, is the uniqueness of this Lewis acid which makes it a promising catalyst in the field of organic synthesis. Copper octoate is commercially available with quite low costs and in the form of solvated in organic solvents in various grades and with different metal content and solvents which can be manufactured upon customer's demand.

Arylmethylene bis(3-hydroxy-2-cyclohexene-1-one) derivatives belong to the family of tetraketones which are used as valuable intermediates for the synthesis of various heterocycles such as acridines, xanthenes, and thiaxanthenes which contain structures including dihydropyridine, pyran, and thiapyran [19]. These compounds have applications in laser technology [20] as well as clinical uses as antioxidant [21], tyrosinase [22], and lipoxygenase [21] inhibitors.

The first report about the synthesis and characterization of this class of compounds was by George Merling and in the course of preparing 1,3-cyclohexanedione from resorcinol [23]. Nevertheless, the principle synthetic avenue to arylmethylene bis(3-hydroxy-2-cyclohexene-1-ones) comprises the condensation of an aldehyde with a two-fold excess of 1,3-cyclohexanedione derivatives. This reaction was utilized for identification and characterization of aldehydes and was carried out in aqueous ethanolic solution catalyzed by piperidine [24].

So far, various reaction conditions have been presented for this reaction including, $CaCl_2$ in chloroform [25], palladium nanoparticles in water [26], urea in water under ultrasonic irradiation [27], $FeCl_3.6H_2O$ and TMSCl in [bmim][BF_4] [28], I_2 in water [29] and ethylenediamine diacetate in THF [30]. Regarding practical, environmental and economic aspects, most of these methods may not be appropriate for industrial applications.

There are also some catalyst-free approaches using water [31], dichloromethane [32] or DMF [33] as solvents and grinding technique [34]. However, long reaction times associated with these catalyst-free reactions, sometimes up to 24 or 48 hours, remarks the necessity of using a catalyst for this reaction.

In this paper, copper octoate has been applied as a homogeneous catalyst for the convenient synthesis of 2,2′-arylmethylenebis(3-hydroxy-5,5-dimethyl-2-cyclohexene-1-ones) (MbHDMC). Copper octoate exhibited pronounced catalytic activity and was easily separated by simple filtration (Scheme 1).

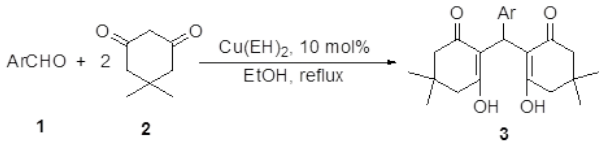

Scheme 1. Synthesis of MbHDMC (3) using copper octoate as catalyst.

Experimental

All the chemicals were purchased from Merck and Sigma-Aldrich companies. Melting points were measured by using the capillary tube method with an Electrothermal 9200 apparatus. ^{1}H-NMR and ^{13}C-NMR spectra were recorded on a Bruker AQS AVANCE-400 MHz spectrometer, using TMS as an internal standard ($CDCl_3$ solution). FT-IR spectra were recorded on the FT-IR Bruker Tensor 27. Elemental analyses (% C, H, N) were carried out by Perkin-Elmer 2400 CHN elemental analyzer.

Synthesis of Copper Octoate

Although this complex is widely available and could be purchased in quite low costs, an example of its preparation has been provided to illustrate the simplicity involved in it which could be counted as another advantage for extending its applications.

To a solution of 2-ethylhexanoic acid (98%, 0.12 mol, 18.00 g) in 100 mL of xylene in a round-bottomed flask, sodium hydroxide (0.12 mol, 5.00 g) solution in 50 mL of water was added. Next, the mixture was stirred and a solution of copper sulfate pentahydrate (0.06 mol, 15.00 g) in 50 mL of water was added drop wise. The mixture was stirred for 1 hour and then the two phases were separated. The organic phase was washed with water and dried by azeotropic distillation in the form of a binary azeotrope of water and xylene, from which the water is removed by distillation using a Dean-Stark apparatus.

General procedure for the synthesis of MbHDMCs using copper octoate as catalyst

To a solution of aldehyde (1 mmol) and dimedone (2 mmol, 0.28 g) in ethanol (5 mL), a solution of copper octoate in xylene (6%, 0.1 mmol, 0.58 g) was added. The solution was refluxed for the amount of time indicated in Table 2. After completion of the reaction as monitored by TLC, using petroleum ether:ethyl acetate (4:1, v:v) as eluent, the reaction mixture was cooled to room temperature and then the precipitated product was simply filtered and washed with ethanol. The catalyst was easily removed to the filtrate in the solvated form in ethanol. For further purification, the products were recrystallized from ethanol. All of the products were known and their physical data were compared with those of authentic samples in the literature and found to be identical.

Physical and spectral data

2,2'-phenylmethylenebis(3-hydroxy-5,5-dimethyl-2-cyclohexene-1-one) (3a)

Mp: 191 °C; FT-IR (KBr): 3423, 2842, 1593, 1498, 1314, 871 cm^{-1}; ^{1}H-NMR (δ, 400 MHz, $CDCl_3$): 1.15 (s, 6H, $2CH_3$), 1.27 (s, 6H, $2CH_3$), 2.31–2.56 (m, 8H, $4CH_2$), 5.54 (s, 1H, CH), 7.08–7.28 (m, 5H, ArH), 9.76 (s, 1H, OH), 11.89 (s, 1H, OH); ^{13}C-NMR (δ, 100 MHz, $CDCl_3$): 26.5, 29.7, 30.1, 32.8, 46.7, 47.4, 116.6, 124.3, 125.5, 128.7, 138.3, 190.4, 190.8; Anal. Calcd. for $C_{23}H_{28}O_4$: C%, 74.97; H%, 7.66. Found: C%, 74.62; H%, 7.71.

2,2'-(4-methoxyphenyl)methylenebis(3-hydroxy-5,5-dimethyl-2-cyclohexene-1-one) (3b)

Mp: 147 °C; FT-IR (KBr): 3596, 1794, 1620, 1403, 1175 cm^{-1}; ^{1}H-NMR (δ, 400 MHz, $CDCl_3$): 1.15 (s, 6H, $2CH_3$), 1.65 (s, 6H, $2CH_3$), 2.34–2.42 (m, 8H, $4CH_2$), 3.81 (s, 3H, OCH_3), 5.81 (s, 1H, CH), 6.61 (d, *J*= 8.1 Hz, 2H, ArH), 6.88 (d, *J*= 8.1 Hz, 2H, ArH), 12.06 (brs, 2H, OH); ^{13}C-NMR (δ, 100 MHz, $CDCl_3$): 26.8, 29.2, 31.0, 31.9, 45.2, 46.8, 55.9, 113.3, 115.7, 127.5, 129.2, 157.1, 189.1, 190.4; Anal. Calcd. for $C_{24}H_{30}O_5$: C%, 72.34; H%, 7.59. Found: C%, 72.24; H%, 7.75.

2,2'-(3-nitrophenyl)methylenebis(3-hydroxy-5,5-dimethyl-2-cyclohexene-1-one) (3c)

Mp: 194-196 °C; FT-IR (KBr): 3394, 2972, 1599, 1379 cm^{-1}; 1H-NMR (δ, 400 MHz, $CDCl_3$): 1.10 (s, 6H, $2CH_3$), 1.05 (s, 6H, $2CH_3$), 2.36-2.58 (m, 8H, $4CH_2$), 5.55 (s, 1H, CH), 7.45-7.50 (m, 2H, ArH), 8.00-8.08 (m, 2H, ArH), 11.85 (brs, 2H, 2OH); ^{13}C-NMR (δ, 100 MHz, $CDCl_3$): 27.22, 29.70, 31.44, 32.85, 46.43, 46.99, 113.12, 121.07, 123.22, 129.16, 133.88, 141.65, 148.46, 189.68, 194.15; Anal. Calcd. for $C_{23}H_{27}NO_6$: C%, 66.81; H%, 6.58; N%, 3.39. Found: C%, 66.73; H%, 6.80; N%, 3.12.

2,2'-(4-nitrophenyl)methylenebis(3-hydroxy-5,5-dimethyl-2-cyclohexene-1-one) (3d)

Mp: 190 °C; FT-IR (KBr): 2962, 1533, 1513, 1375, 1345 cm^{-1}; ^{1}H-NMR (δ, 400 MHz, $CDCl_3$): 1.11(s, 6H, $2CH_3$), 1.18 (s, 6H, $2CH_3$), 2.47 (m, 8H, $4CH_2$), 5.58 (s, 1H, CH), 7.22 (d, *J*= 8.9 Hz, 2H, ArH), 8.17 (d, *J*= 8.9 Hz, 2H, ArH), 9.77 (s, 1H, OH), 11.79 (s, 1H, OH); ^{13}C-NMR (δ, 100 MHz, $CDCl_3$): 27.0, 29.6, 32.5, 33.3, 45.4, 47.0, 114.8, 123.1, 127.8, 146.0, 146.4, 189.8, 190.8; Anal. Calcd. for $C_{23}H_{27}NO_6$: C%, 66.81; H%, 6.58; N%, 3.39. Found: C%, 66.65; H%, 6.83; N%, 3.24.

2,2'-(4-methylphenyl)methylenebis(3-hydroxy-5,5-dimethyl-2-cyclohexene-1-one) (3e)

Mp: 142 °C; FT-IR (KBr): 3421, 2963, 2640, 1685, 1477, 1383, 1160, 892 cm^{-1}; ^{1}H-NMR (δ, 400 MHz, $CDCl_3$): 1.15 (s, 6H, $2CH_3$), 1.24 (s, 6H, $2CH_3$), 2.32–2.54 (m, 8H, $4CH_2$), 5.46 (s, 1H, CH), 2.76 (s, 3H, CH_3), 6.91–7.24 (m, 3H, ArH), 11.58 (s, 1H, OH), 11.92 (s, 1H, OH); Anal. Calcd. for $C_{24}H_{30}O_4$: C%, 75.36; H%, 7.91. Found: C%, 75.37; H%, 7.69.

2,2'-(4-N,N-dimethylaminophenyl)methylenebis(3-hydroxy-5,5-dimethyl-2-cyclohexene-1-one) (3f)

Mp: 195-197 °C; FT-IR (KBr): 3132, 1605, 1521, 1377, 1315, 1268, 811 cm^{-1}; ^{1}H-NMR (δ, 400 MHz, $CDCl_3$): 0.99 (s, 6H, $2CH_3$), 1.28 (s, 6H, $2CH_3$), 2.30–2.50 (m, 8H, $4CH_2$), 3.09 (s, 6H, $N(CH_3)_2$), 5.46 (s, 1H, CH), 6.69 (d, *J*= 8.4 Hz, 2H, ArH), 6.98 (d, *J*= 8.4 Hz, 2H, ArH), 9.53 (s, 1H, OH),11.95 (s, 1H, OH); Anal. Calcd. for $C_{25}H_{33}NO_4$: C%, 72.96; H%, 8.08; N%, 3.40. Found: C%, 72.90; H%, 8.23; N%, 3.24.

2,2'-(4-hydroxyphenyl)methylenebis(3-hydroxy-5,5-dimethyl-2-cyclohexene-1-one) (3g)

Mp: 190 °C; FT-IR (KBr): 3425, 3083, 1595, 1498, 1374, 1322 cm^{-1}; ^{1}H-NMR (δ, 400 MHz, $CDCl_3$): 1.08 (s, 6H, $2CH_3$), 1.22 (s, 6H, $2CH_3$), 2.45 (m, 8H, $4CH_2$), 5.41 (s, 1H, CH), 6.82 (d, *J*= 8.8 Hz, 2H, ArH),

7.01 (d, J= 8.8 Hz, 2H, ArH), 9.48 (s, 1H, OH), 11.91 (brs, 2H, 2OH); ^{13}C-NMR (δ, 100 MHz, $CDCl_3$): 27.4, 29.4, 31.2, 32.0, 46.7, 47.2, 115.4, 115.9, 128.0, 129.5, 153.6, 189.5, 190.7; Anal. Calcd. for $C_{23}H_{28}O_5$: C%, 71.85; H%, 7.34. Found: C%, 71.67; H%, 7.78.

2,2′-(4-bromophenyl)methylenebis(3-hydroxy-5,5-dimethyl-2-cyclohexene-1-one) (3h)

Mp: 173-176 °C; FT-IR (KBr): 3463, 2994, 2865, 1743, 1731, 1601 cm^{-1}; ^{1}H-NMR (δ, 400 MHz, $CDCl_3$): 1.14 (s, 6H, $2CH_3$), 1.28 (s, 6H, $2CH_3$), 2.19–2.45 (m, 8H, $4CH_2$), 5.49 (s, 1H, CH), 7.00 (d, *J*= 6.6 Hz, 2H, ArH), 7.39 (d, *J*= 6.6 Hz, 2H, ArH), 11.94 (brs, 2H, 2OH); ^{13}C-NMR (δ, 100 MHz, $CDCl_3$): 27.41, 29.66, 31.23, 32.48, 46.44, 47.14, 115.56, 119.63, 128.65, 131.89, 137.22, 189.45, 190.75; Anal. Calcd. for $C_{23}H_{27}BrO_4$: C%, 61.75; H%, 6.08. Found: C%, 61.42; H%, 6.12.

Results and Discussion

Initially, benzaldehyde was selected as a typical aromatic aldehyde in order to optimize parameters such as the amount of catalyst, solvent, and temperature. The reaction between benzaldehyde (1 mmol) and dimedone (2 mmol) was carried out in ethanol and under reflux. After one hour, the product was obtained in 69% yield. However, in the presence of 15 mol% of copper octoate as catalyst, the yield of the target compound (**3a**) increased to 90% and the reaction time decreased to 25 min which highlights the effect of the catalyst. To optimize the amount of catalyst, the model reaction was carried out in the presence of different quantities of catalyst. As shown in Table 1, the best result was with 10 mol% of the catalyst. In the next step, we switched to decide the best reaction medium by running the model reaction in other solvents like acetonitrile and chloroform, but no improvement was observed in reaction profiles. Various temperatures were also examined disclosing the fact that the reaction shows a great dependence on temperature and higher temperatures are preferable in terms of reaction times and yields.

With these initial results in hand, we next examined the generality of this method using different aromatic aldehydes with various substitution patterns. These results are collected in Table 2. Under the optimized conditions, irrespective of the substituent present on aromatic ring, the corresponding products were obtained with high yields and purity by simple filtration.

For many years, these target compounds were considered as tetraketones. However, according to spectral data and X-ray diffraction studies [33], a keto-enol form has now been assigned to this class of compounds as the major structure. For example, in ^{1}H-NMR spectra of **3a**, three singlet protons have been appeared in 11.89, 9.76, and 5.54 ppm which are attributed to hydroxyl protons and the benzylic proton connected to linker carbon, respectively. The singlet form of these peaks negates the presence of any adjacent proton to the aforementioned protons, which occurs in tetraketone frameworks. In addition, hydroxyl absorption in 3423 cm^{-1} and carbonyl absorption in 1593 cm^{-1} in the FT-IR spectra, are other evidences which give more clarification to recommended keto-enol structure.

Table 1. Optimization of the conditions for the model reaction of benzaldehyde with dimedone.

Entry	Amount of catalyst (mol%)	Solvent	Temperature (°C)	Time (min)	Yield (%)
1	0	EtOH	Reflux	60	69
2	5	EtOH	Reflux	40	90
3	10	EtOH	Reflux	24	91
4	15	EtOH	Reflux	25	90
5	20	EtOH	Reflux	25	88
6	10	CH_3CN	Reflux	32	85
7	10	$CHCl_3$	Reflux	30	84
8	10	EtOH	25	60	87
9	10	EtOH	40	45	88
10	10	EtOH	60	30	91

Table 2. Synthesis of various MbHDMCs catalyzed by copper octoate[a].

Entry	Ar	Product	Time (min)	Yield (%)	mp (°C)	
					Found	Reported
1	C_6H_5	**3a**	24	91	191	190-191 [35]
2	4-$OMeC_6H_4$	**3b**	35	88	147	146-148 [25]
3	3-$NO_2C_6H_4$	**3c**	16	89	194-196	190-191 [27]
4	4-$NO_2C_6H_4$	**3d**	20	90	190	189 [35]
5	4-MeC_6H_4	**3e**	50	91	142	139-141 [25]
6	4-$N(Me)_2C_6H_4$	**3f**	27	88	195-197	195-196 [34]
7	4-OHC_6H_4	**3g**	45	89	190	189 [35]
8	4-BrC_6H_4	**3h**	40	88	173-176	172-174 [28]

[a]Reaction Conditions: aldehyde (1 mmol), dimedone (2 mmol), 6% xylene solution of copper octoate (0.1 mmol, 0.58 g), EtOH (5 mL), reflux.

On the other hand, according to the symmetrical appearance of the structures of the products, it is initially expected that ^{1}H-NMR spectrum of these compounds would be clear and uncrowded ones exhibiting two hydroxyl protons in the same chemical shift; while in fact, the number of signals are more than what was anticipated and hydroxyl groups appeared at δ 11.89 and 9.76 ppm. These distinguished chemical shifts disclose the asymmetric character of the structure of the product which could be simply explained by the intramolecular hydrogen bonds, decreasing the asymmetry of the molecule effectively (Figure 2). Indeed, the formation of intramolecular hydrogen bonds restricts the rotation around the methylene bridge and locks the molecule in a rigid asymmetric form in which one of the hydroxyl groups is settled close to the benzylic proton and probably corresponds to the high-field signal while the other hydroxyl proton next to the Ar group is related to the low-field signal. In other words, the methylene bridge acts as a chiral center inducing a diastereotopic relationship between the hydroxyl groups. Kaupp et al. demonstrated the presence of intramolecular hydrogen bonds as two almost identical O-H…O hydrogen bridges by B3LYP/6-31G calculations. The formation of these hydrogen bridges was attributed to molecular tendency for minimizing its energy levels [35]. Similar interpretations were also made by several groups to illustrate the presence of intramolecular hydrogen bonds in bis(coumarin) derivatives [36-38] (Figure 2).

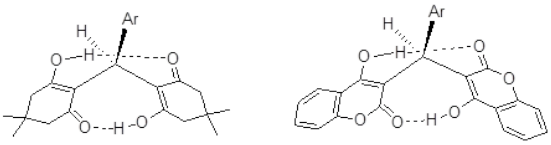

Figure 2. Intramolecular hydrogen bonding in MbHDMC and biscoumarin derivatives.

A possible mechanism for this reaction is demonstrated in Figure 3. Lewis acid-catalyzed Knoevenagel condensation of aldehyde (**1**) and dimedone (**2**) results in the formation of the intermediate (**4**), which on addition of the second molecule of dimedone, the target MbHDMC (**3**) is formed. The blockage of the reaction at this stage, the reluctance for dehydration of (**3**), and formation of the corresponding xanthene could be attributed to the mild essence of copper octoate and also the fact that the desired product (**3**) gradually precipitates from the reaction solution and practically interrupts the function of homogeneous copper octoate catalyst.

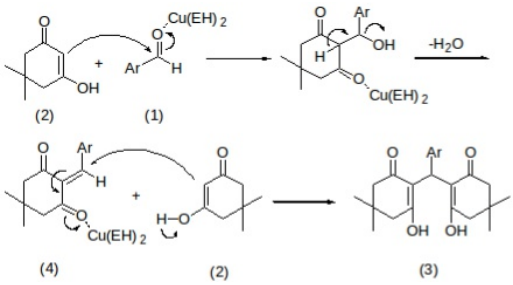

Figure 3. Plausible mechanism for the copper octoate-catalyzed synthesis of MbHDMCs.

After completion of each reaction, the reaction mixture was cooled to room temperature and the precipitated product was simply filtered and washed with ethanol. For evaluating the reusability of the catalyst, the filtrate was heated to remove the excess of ethanol and reduce the volume to approximately 5.6 mL (the amount of ethanol required as solvent for the next run plus the xylene solution of the copper octoate). To the concentrated solution remained, the starting materials of the model reaction were simply added and the resulted solution was heated to reflux. As it is exhibited in Table 3, the recycled catalyst solution promoted reactions in a similar manner without significant loss of activity.

In order to prove the merit of copper octoate functioning as a homogeneous catalyst in the synthesis of MbHDMCs,the results obtained for the model reaction in the present work has been compared with previously reported methods in Table 4.

As it is obviously illustrated, the yield obtained using copper octoate as catalyst is almost comparable to other catalysts and conditions but reaction time has been shortened remarkably to amount which is rarely achieved by other approaches presented.

Table 3. Evaluating the reusability of the catalyst.

Run	Yield (%)
1	91
2	88
3	89
4	85

Table 4. Comparison of the efficiency of copper octoate with other reagents and conditions for the synthesis of (**3a**)

Entry	Catalyst	Condition/Solvent	Time (h)	Yield (%)	Reference
1	Urea	US, 50 ^{0}C/H_2O	1	94	[27]
2	ZnO	reflux, CH_3CN	12	92	[39]
3	$HClO_4$-SiO_2	reflux, H_2O	0.5	91	[40]
4	EDDA[a]	reflux, THF	4	88	[30]
5	N/A	Ball-milling	1	100	[35]
6	N/A	100 ^{0}C, neat grinding	0.67	86	[34]
7	N/A	RT, neat RT, CH_2Cl_2	24	69	[32]
8	Pd nanoparticles	reflux, H_2O	0.3	88	[26]
9	$CaCl_2$	RT, $CHCl_3$	13	69	[25]
10	KF/Al_2O_3	grinding	0.33-0.66	86	[41]
11	$FeCl_3.6H_2O$+TMSCl	RT, neat 80 ^{0}C	6	89	[28]
12	N/A	[bmim][BF_4] 80 ^{0}C/DMF	1	80	[33]
13	$Cu(EH)_2$	reflux, EtOH	0.4	91	[b]

[a] Ethylenediamine diacetate.

[b] This work.

Conclusion

In summary, copper octoate as an extensively used industrial reagent has been introduced as a mild Lewis acid catalyst for the synthesis of MbHDMCs. Fine tuning of reaction conditions such as the strength of the catalyst and even solvent plays a critical role in controlling progress of the reaction in the desired level since harsh reaction conditions may result in cyclodehydration and formation of the byproduct of xanthene. In this reaction, the dramatic effect of copper octoate being acidic enough to accelerate the reaction up to very short times in one hand and mild enough to terminate reaction after formation of Michael adducts on the other hand, is quite noticeable. This behavior could be useful in lots of other synthetic processes. In fact, non-corrosive and green character, low cost, and commercial availability are features making it a superior choice as catalyst in organic transformations specially those having an emphasize on the homogeneity of the catalyst.

Acknowledgments

The authors are thankful to Alzahra Research Council for partial financial support.

References

[1] Hegedus LS. Transition metals in the synthesis of complex organic molecules. 3rd ed. Sausalito, Calif: University Science Books; 2010. 459 p. ISBN: 9781891389597.

[2] Bates R. Organic synthesis using transition metals. 2nd ed. Chichester, West Sussex: Wiley; 2012. 446 p. ISBN: 9781119978930.

[3] Barnes HM, Amburgey TL, Sanders MG. Performance of copper naphthenate and its analogs as ground contact wood preservatives. Bioresource Technology. 2005 Jul;96(10):1131–5. DOI: 10.1016/j.biortech.2004.10.003.

[4] Kamimoto M, Sakamoto R, Negishi A, Takahashi Y, Hirabayashi M. Thermoanalytical investigation of YBa2Cu3O7-y superconductor. IV. Mechanism of perovskite formation from various starting materials. Thermochimica Acta. 1989 Apr;142(2):281–90. DOI: 10.1016/0040-6031(89)85025-7.

[5] Nasu H, Makida S, Imura T, Osaka Y. Ba2YCu3O x films withT c (end) > 80 K prepared by the pyrolysis of 2-ethylhexanoates. Journal of Materials Science Letters. 1988 Aug;7(8):858–60. DOI: 10.1007/BF00723786.

[6] Nasu H, Makida S, Kato T, Ibara Y, Imura T, Osaka Y. Superconducting Y-Ba-Cu-O films with Tc>70K prepared by thermal decomposition technique of Y-, Ba-, and Cu-2ethylhexanoates. Chemistry Letters. 1987;(12):2403–4. DOI: 10.1246/cl.1987.2403.

[7] Li QF, Lu K, Yang Q, Jin R. The effect of different metallic catalysts on the coreaction of cyanate/epoxy. Journal of Applied Polymer Science. 2006 May 5;100(3):2293–302. DOI: 10.1002/app.22882.

[8] Kolomeyer GG, Oyloe JS. Catalyst system and process for rearrangement of epoxides to allylic alcohols [Internet]. Google Patents; 2004. Available from: http://www.google.com/patents/US6835686

[9] Lalic G, Aloise AD, Shair MD. An Exceptionally Mild Catalytic Thioester Aldol Reaction Inspired by Polyketide Biosynthesis. Journal of the American Chemical Society. 2003 Mar;125(10):2852–3. DOI: 10.1021/ja029452x.

[10] Baran PS, Maimone TJ, Richter JM. Total synthesis of marine natural products without using protecting groups. Nature. 2007 Mar 22;446(7134):404–8. DOI: 10.1038/nature05569.

[11] Baran PS, Richter JM, Lin DW. Direct Coupling of Pyrroles with Carbonyl Compounds: Short Enantioselective Synthesis of (S)-Ketorolac. Angewandte Chemie International Edition. 2005 Jan 14;44(4):609–12. DOI: 10.1002/anie.200462048.

[12] Baran PS, DeMartino MP. Intermolecular Oxidative Enolate Heterocoupling. Angewandte Chemie International Edition. 2006 Oct 27;45(42):7083–6. DOI: 10.1002/anie.200603024.

[13] Rao VDN. Oxidation catalysts [Internet]. Google Patents; 1987. Available from: http://www.google.com/patents/US4670020

[14] Raje N, Naik VR, Reddy AVR. Thermal decomposition mechanism of synthesized copper octoate. Journal of Thermal Analysis and Calorimetry. 2013 Apr;112(1):187–92. DOI: 10.1007/s10973-012-2748-x.

[15] Doyle A, Felcman J, Gambardella MT do P, Verani CN, Tristão MLB. Anhydrous copper(II) hexanoate from cuprous and cupric oxides. The crystal and molecular structure of Cu2(O2CC5H11)4. Polyhedron. 2000 Dec;19(26-27):2621–7. DOI: 10.1016/S0277-5387(00)00568-4.

[16] Lah N, Giester G, Lah J, Šegedin P, Leban I. Copper(II) carboxylates with 2-aminopyridine. Synthesis, characterization and a study of the dimer–monomer equilibrium in acetonitrile solutions by VIS-spectroscopic and microcalorimetric titrations. New Journal of Chemistry. 2001;25(5):753–9. DOI: 10.1039/B009807H.

[17] Raju R, Prasad K. Synthetic applications of 2-ethylhexanoic acid derived reagents. Tetrahedron. 2012 Feb;68(5):1341–9. DOI: 10.1016/j.tet.2011.10.078.

[18] Fuller PH, Chemler SR. Copper(II) Carboxylate-Promoted Intramolecular Carboamination of Alkenes for the Synthesis of Polycyclic Lactams. Organic Letters. 2007 Dec;9(26):5477–80. DOI: 10.1021/ol702401w.

[19] Li-Bin L, Tong-Shou J, Li-Sha H, Meng L, Na Q, Tong-Shuang L. The Reaction of Aromatic Aldehydes and 1,3-Cyclohexanedione in Aqueous Media. E-Journal of Chemistry. 2006;3(3):117–21. DOI: 10.1155/2006/686538.

[20] Banerjee A, Mukherjee AK. Chemical Aspects of Santalin as a Histological Stain. Biotechnic & Histochemistry. 1981 Jan;56(2):83–5. DOI: 10.3109/10520298109067286.

[21] Maharvi GM, Ali S, Riaz N, Afza N, Malik A, Ashraf M, et al. Mild and efficient synthesis of new tetraketones as lipoxygenase inhibitors and antioxidants. Journal of Enzyme Inhibition and Medicinal Chemistry. 2008 Jan;23(1):62–9. DOI: 10.1080/14756360701408754.

[22] Khan KM, Maharvi GM, Khan MTH, Jabbar Shaikh A, Perveen S, Begum S, et al. Tetraketones: A new class of tyrosinase inhibitors. Bioorganic & Medicinal Chemistry. 2006 Jan;14(2):344–51. DOI: 10.1016/j.bmc.2005.08.029.

[23] Merling G. Ueber Dihydroresorcin. Justus Liebig's Annalen der Chemie. 1894;278(1):20–57. DOI: 10.1002/jlac.18942780103.

[24] Horning EC, Horning MG. METHONE DERIVATIVES OF ALDEHYDES. The Journal of Organic Chemistry. 1946 Jan;11(1):95–9. DOI: 10.1021/jo01171a014.

[25] Ilangovan A, Muralidharan S, Sakthivel P, Malayappasamy S, Karuppusamy S, Kaushik MP. Simple and cost effective acid catalysts for efficient synthesis of 9-aryl-1,8-dioxooctahydroxanthene. Tetrahedron Letters. 2013 Feb;54(6):491–4. DOI: 10.1016/j.tetlet.2012.11.058.

[26] Saha M, Pal AK, Nandi S. Pd(0) NPs: a novel and reusable catalyst for the synthesis of bis(heterocyclyl)methanes in water. RSC Advances. 2012;2(16):6397. DOI: 10.1039/C2RA20445B.

[27] Li J-T, Li Y-W, Song Y-L, Chen G-F. Improved synthesis of 2,2′-arylmethylene bis(3-hydroxy-5,5-dimethyl-2-cyclohexene-1-one) derivatives catalyzed by urea under ultrasound. Ultrasonics Sonochemistry. 2012 Jan;19(1):1–4. DOI: 10.1016/j.ultsonch.2011.05.001.

[28] Fan X, Li Y, Zhang X, Hu X, Wang J. FeCl3.6H2O catalyzed condensation of aromatic aldehydes with 5,5-dimethyl-1,3-cyclohexanedione in ionic liquids. Chinese Journal of Organic Chemistry. 2005;25:1482–6.

[29] Kidwai M, Bansal V, Mothsra P, Saxena S, Somvanshi RK, Dey S, et al. Molecular iodine: A versatile catalyst for the synthesis of bis(4-hydroxycoumarin) methanes in water. Journal of Molecular Catalysis A: Chemical. 2007 May;268(1-2):76–81. DOI: 10.1016/j.molcata.2006.11.054.

[30] Jung D, Lee Y, Kim S, Lyoo W. New and General Methods for the Synthesis of Arylmethylene Bis(3-Hydroxy-2-Cyclohexene-1-Ones) and Xanthenediones by EDDA and In(OTf) 3 -Catalyzed One-Pot Domino Knoevenagel/Michael or Koevenagel/Michael/Cyclodehydration Reactions. Bulletin of the Korean Chemical Society. 2009 Sep 20;30(9):1989–95. DOI: 10.5012/bkcs.2009.30.9.1989.

[31] Bayat M, Imanieh H, Hossieni SH. Synthesis of 2,2′-arylmethylene bis (3-hydroxy-5,5-dimethyl-2-cyclohexene-1-one) in aqueous medium at room temperature. Chinese Chemical Letters. 2009 Jun;20(6):656–9. DOI: 10.1016/j.cclet.2008.12.050.

[32] Rohr K, Mahrwald R. Catalyst-free tandem aldol condensation/Michael addition of 1,3-cyclohexanediones with enolizable aldehydes. Bioorganic & Medicinal Chemistry Letters. 2009 Jul;19(14):3949–51. DOI: 10.1016/j.bmcl.2009.03.040.

[33] Shi D, Wang Y, Lu Z, Dai G. Condensation of Aromatic Aldehydes with Acidic Methylene Compounds without Catalyst. Synthetic Communications. 2000 Feb;30(4):713–26. DOI: 10.1080/00397910008087374.

[34] Jin T, Zhang J, Wang A, Li T. Solid-State Condensation Reactions Between Aldehydes and 5,5-Dimethyl-1,3-cyclohexanedione by Grinding at Room Temperature. Synthetic Communications. 2005 Sep;35(17):2339–45. DOI: 10.1080/00397910500187282.

[35] Kaupp G, Reza Naimi-Jamal M, Schmeyers J. Solvent-free Knoevenagel condensations and Michael additions in the solid state and in the melt with quantitative yield. Tetrahedron. 2003 May;59(21):3753–60. DOI: 10.1016/S0040-4020(03)00554-4.

[36] Hamdi N, Puerta MC, Valerga P. Synthesis, structure, antimicrobial and antioxidant investigations of dicoumarol and related compounds. European Journal of Medicinal Chemistry. 2008 Nov;43(11):2541–8. DOI: 10.1016/j.ejmech.2008.03.038.

[37] Labbe-Bois R, Laruelle C, Godfroid JJ. Quantitative structure-activity relations for dicoumarol antivitamins K in the uncoupling of mitochondrial oxidative phosphorylation. Journal of Medicinal Chemistry. 1975 Jan;18(1):85–90. DOI: 10.1021/jm00235a019.

[38] Laruelle C, Godfroid J-J. A stereodynamic investigation of antivitamins K in the dicoumarol series. II. Differentiation between the two hydroxyl groups by the nuclear Overhauser effect. Canadian Journal of Chemistry. 1976 Mar;54(5):813–6. DOI: 10.1139/v76-117.

[39] Maghsoodlou MT, Habibi-Khorassani SM, Shahkarami Z, Maleki N, Rostamizadeh M. An efficient synthesis of 2,2′-arylmethylene bis(3-hydroxy-5,5-dimethyl-2-cyclohexene-1-one) and 1,8-dioxooctahydroxanthenes using ZnO and ZnO–acetyl chloride. Chinese Chemical Letters. 2010 Jun;21(6):686–9. DOI: 10.1016/j.cclet.2010.02.005.

[40] Kantevari S, Bantu R, Nagarapu L. HClO4–SiO2 and PPA–SiO2 catalyzed efficient one-pot Knoevenagel condensation, Michael addition and cyclo-dehydration of dimedone and aldehydes in acetonitrile, aqueous and solvent free conditions: Scope and limitations. Journal of Molecular Catalysis A: Chemical. 2007 May;269(1-2):53–7. DOI: 10.1016/j.molcata.2006.12.039.

[41] Jin T-S, Wang A-Q, Ma H, Zhang J-S, Li T-S. The Reaction of Aromatic Aldehydes and 5,5-Dimethyl-1,3-cyclohexanedione under Solvent-Free Grinding Conditions. ChemInform [Internet]. 2006 May 30 [cited 2015 Mar 18];37(22). Available from: http://doi.wiley.com/10.1002/chin.200622038. DOI: 10.1002/chin.200622038.

JOTCSA, volume 2, issue 4 (2015), pp. 12-21

Research Article

http://dergipark.ulakbim.gov.tr/jotcsa

Synthesis and Comparative Antibacterial Studies of some Benzylidene Monosaccharide Benzoates

Mohammed M. Matin[1]*, M.M.H. Bhuiyan[1], Md. Manir Hossain[1], and Mohammad Harun Or Roshid[2]

[1] Organic Research Laboratory, Department of Chemistry, University of Chittagong, Chittagong-4331, Bangladesh.

[2] Department of Anesthesia and Intensive Care, Chittagong Medical College, Chittagong-4203, Bangladesh.

E-mail: mahbubchem@cu.ac.bd, Tel. no.: 8801716839689

Abstract: Methyl α-D-glucopyranoside on reaction with benzaldehyde followed by direct dimolar benzoylation afforded 4,6-*O*-benzylidene-protected 2,3-di-*O*-benzoate **3** in good yield. Regioselective monobenzoylation of methyl α-D-mannopyranoside employing dibutyltin oxide method furnished 3-*O*-benzoate **5**. Compound **5**, on treatment with excess benzaldehyde followed by direct benzoylation, provided 2,3-di-*O*-benzoate **7** in high yield. *In vitro* antibacterial activity studies of the synthesized compounds along with the precursor materials (**1-7**) were evaluated against ten bacterial pathogens. The structure activity relationship study revealed that the benzoyl mannopyranosides (**5-7**) exhibited more antibacterial inhibitory property as compared to that of glucopyranosides (**2-3**).

Submitted: February 08, 2015. **Revised:** March 10, 2015. **Accepted:** March 10, 2015.

Keywords: Monosaccharide, benzoylation, antibacterial activity, structure activity relationship (SAR).

Introduction

Monosaccharides are wide spread in nature, being a component of some plant glycosides and bacterial polysaccharides of immunological importance [1-2]. Monosaccharide derivatives, especially acylated monosaccharides (esters), have synthetic utility as versatile intermediates in the syntheses of many natural products and their analogues which have great medicinal importance [3-4]. Various methods for acylation of monosaccharides have so far been developed and employed successfully such as direct acylation [5-6], protection-deprotection technique [7], organotin (bistributyltin oxide or dibutyltin oxide) mediated regioselective acylation [8-10] *etc*. Yet, regioselective acylation (esterification) is a prominent challenge as monosaccharides contain several hydroxyl groups of similar reactivity. In this context, enzyme catalyzed acylation [11] and microwave assisted acylation [12] were also investigated in the past decade. In the present synthetic strategy, we employed direct acylation technique for both methyl α-D-glucopyranoside (**1**) and methyl α-D-mannopyranoside (**4**). We have also used dibutyltin oxide method for the regioselective 3-*O*-benzoylation of mannopyranoside **4**.

The emergence of multiple antibiotic resistant pathogenic bacteria represents a growing threat to human health worldwide. Thus, search for new antibacterial agents with novel mode of action represents a major target in chemotherapy [13]. Acylated sugars (esters) have been widely used as cosmetic and pharmaceutical industries for many years because they are considered biocompatible, biodegradable, and nontoxic [14-15].

In ^{1}H NMR analysis of **1** in DMSO-d_6, aromatic protons appear at 8.58, 8.28, 8.02, 7.59, 7.11, 7.05 ppm as a doublet, singlet, multiple, triplet, doublet and doublet, respectively. The OH proton appear at 10.28 ppm as singlet. The ^{1}H NMR spectra of the compounds **2** and **3** are somewhat broader than corresponding signals in the compound **1** due to aggregation of the phthalocyanine isomers which is frequently encountered at the concentrations used for NMR spectroscopy. The inner NH protons of **2** were also identified in the ^{1}H NMR spectra with a broad chemical shift at -4.03 ppm.

In ^{13}C NMR analysis of **1** in DMSO-d_6, aromatic carbons appear at 158.53, 146.53, 135.11, 130.37, 129.48, 129.01, 128.38, 128.33, 127.87, 126.51, 126.11, 123.50, 123.16, 120.22, and 116.35 ppm, C-OH group appeared at 153.49 ppm, nitrile carbons appeared at 115.72 and 114.87 ppm, respectively.

In the EI^{+} mass spectrum of **1**, the presence of the characteristic molecular ion peak at m/z 298.0 $[M]^{+}$ confirmed the proposed structure. In the case of **2**, the molecular ion peak was found at m/z 1233.5 $[M+K]^{+}$ according to MALDI-TOF spectrum (Fig. 1). Also, the molecular ion peak for compound **3** found at m/z = 1260.7 $[M+2]^{+}$. The elemental analyses were satisfactory.

Materials and Methods

Chemicals and Apparatus

FT-IR spectra were recorded on an FT-IR spectrometer (Shimadzu, IR Prestige-21) using $CHCl_3$ mulls. Thin layer chromatography (TLC) was performed on Kieselgel GF_{254} and visualization was accomplished by spraying the plates with 1% H_2SO_4 followed by heating the plates at 150-200 ^{0}C until coloration took place. ^{1}H (400 MHz) and ^{13}C (100 MHz) NMR spectra were recorded using $CDCl_3$ as a solvent. Chemical shifts were reported in δ unit (ppm) with reference to TMS as an internal standard and *J* values are given in Hz. Melting points (mp) were determined on an Electrothermal melting point apparatus and are uncorrected. Evaporations were performed under diminished pressure on a Büchi rotary evaporator. All reagents used were commercially available (Aldrich) and were used as received unless otherwise specified.

Synthesis

Methyl 4,6-*O*-benzylidene-α-D-glucopyranoside (2): Benzaldehyde (3.0 g, 28.27 mmol) was added to methyl α-D-glucopyranoside (1) (0.4 g, 2.06 mmol) followed by addition of anhydrous zinc chloride (1.0 g, 7.337 mmol) at room temperature. The reaction mixture was stirred for 12 h and filtered through Celite® 545. Ice was added to the filtrate with constant shaking and the mixture was extracted several times with *n*-hexane to remove unreacted benzaldehyde. The aqueous layer was then extracted with ethyl acetate (3×5 mL) with occasional warming. The organic layer was dried ($MgSO_4$), and concentrated under reduced pressure to yield a residue which, upon chromatographic purification with *n*-hexane/ethyl acetate (1/2, v:v), yielded the title compound **2** (0.401 g, 69%) as a white crystalline solid, mp 162-163 °C (lit. [22], mp 163-164 °C).

R_f = 0.48 (*n*-hexane/ethyl acetate = 1/2, v/v). FT-IR ($CHCl_3$, v, cm^{-1}): 3310-3400 (OH). ^{1}H NMR (400 MHz, $CDCl_3$, δ, ppm): 7.53-7.47 (2H, m, Ar-H), 7.42-7.35 (3H, m, Ar-H), 5.54 (1H, s, PhCH-), 4.80 (1H, d, *J*= 4.0 Hz, H-1), 4.30 (1H, dd, *J*= 9.7 and 4.4 Hz, H-6a), 3.94 (1H, dd, *J*= 9.3 and 9.2 Hz, H-3), 3.82 (1H, ddd, *J*= 10.3, 9.2 and 4.4 Hz, H-5), 3.75 (1H, dd, *J*= 10.3 and 9.7 Hz, H-6b), 3.64 (1H, dd, *J*= 9.2 and 4.0 Hz, H-2), 3.50 (1H, dd, *J*= 9.3 and 9.2 Hz, H-4), 3.47 (3H, s, OCH_3). ^{13}C NMR (100 MHz, $CDCl_3$): δ 137.1 (Ar-C), 129.3, 128.3, 126.3 (Ar-CH), 102.0 (PhCH-), 99.7 (C-1), 80.8 (C-4), 72.9 (C-2), 71.9 (C-3), 68.9 (C-6), 62.4 (C-5), 55.6 (OCH_3).

Methyl 4,6-*O*-benzylidene-2,3-di-*O*-benzoyl-α-D-glucopyranoside (3): A solution of compound **2** (0.3 g, 1.281 mmol) in dry pyridine (1 mL) was cooled to 0 ^{0}C whereupon benzoyl chloride (0.396 g, 2.817 mmol) and DMAP (cat.) were added to it. The mixture was stirred overnight at room temperature. Usual work-up and silica gel column chromatography furnished the di-*O*-benzoyl derivative, 3 (0.521 g, 92%) as a crystalline solid. Recrystallization from ethyl acetate-*n*-hexane gave the analytically pure sample as colorless needles, mp 146-148 °C. R_f = 0.51 (n-hexane/ethyl acetate = 4/1, v/v). FT-IR ($CHCl_3$, v, cm^{-1}): 1735, 1719 (CO). ^{1}H NMR (400 MHz, $CDCl_3$, δ, ppm): 7.81-8.05 (5H, m, Ar-H), 7.31-7.48 (6H, m, Ar-H), 7.21-7.30 (4H, m, Ar-H), 6.02 (1H, t, *J*= 9.8 Hz, H-3), 5.52 (1H, s, PhCH-), 5.21 (1H, dd, *J*= 9.8 and 3.6 Hz, H-2), 5.13 (1H, d, *J*= 3.6 Hz, H-1), 4.28-4.32 (1H, m, H-5), 4.03 (1H, t, *J*= 9.7 Hz, H-4), 3.78-3.87 (2H, m, H-6a and H-6b), 3.37 (3H, s, OCH_3).

Methyl 3-*O*-benzoyl-α-D-mannopyranoside (5): To a solution of methyl α-D-mannopyranoside (**4**) (0.3 g, 1.545 mmol) in dry methanol (10 mL) was added dibutyltin oxide (Bu_2SnO) (0.423 g, 1.699 mmol) and the mixture was heated under reflux. After 2 h the reaction mixture became homogeneous and clear. The mixture was then refluxed for an additional hour and the solvent was evaporated off *in vacuo* to leave a white solid. The solid tin complex was suspended in dry 1,4-dioxane (3 mL) and benzoyl chloride (0.239 g, 1.70 mmol) was slowly added to this solution, with stirring, at room temperature. The solution became clear upon addition of benzoyl chloride and stirring was continued for 4 h. The solvent was evaporated off in vacuo to leave a syrupy mass, which was subjected to column chromatography (chloroform/methanol = 6/1, v/v) to give 3-*O*-benzoate **5** (0.313 g, 68%) as a thick syrup [11].
R_f = 0.48 (chloroform/methanol = 4/1, v/v). FT-IR ($CHCl_3$, v, cm^{-1}): 3260-3350 (br OH), 1746 (CO). ^{1}H NMR (400 MHz, $CDCl_3$, δ, ppm): 7.55-7.73 (5H, m, Ar-H), 6.07 (1H, dd, *J*= 10.0 and 3.1 Hz, H-3), 4.62 (1H, d, *J*= 1.5 Hz, H-1), 4.22 (1H, dd, *J*= 3.1 and 1.5 Hz, H-2), 4.13 (1H, dd, *J*= 12.1 and 5.2 Hz, H-6a), 3.91-3.97 (1H, m, H-5), 3.88 (1H, app t, *J*= 9.8 Hz, H-4), 3.75 (1H, dd, *J*= 12.1 and 2.0 Hz, H-6b), 3.16 (3H, s, OCH_3).

Methyl 3-*O*-benzoyl-4,6-*O*-benzylidene-α-D-mannopyranoside (6): A solution of the 2,4,6-triol **5** (0.4 g, 1.341 mmol) in dry benzaldehyde (3.0 g, 28.27 mmol) was treated with anhydrous zinc chloride (1.0 g, 7.337 mmol) at room temperature. The reaction mixture was stirred at this temperature overnight and filtered through celite. Usual work-up as described for compound **2** and chromatographic purification (*n*-hexane/ethyl acetate = 1/2, v/v) yielded the title compound **6** (0.389 g, 75%) as white needles, mp 135-136 °C. R_f = 0.45 (*n*-hexane/ethyl acetate = 3/1, v/v). FT-IR ($CHCl_3$, v, cm^{-1}): 3290-3500 (br OH), 1735 (CO). ^{1}H NMR (400 MHz, $CDCl_3$, δ, ppm): 8.05 (2H, d, *J*= 8.1 Hz, Ar-H), 8.05 (1H, t, *J*= 7.6 Hz, Ar-H), 7.39-7.46 (5H, m, Ar-H), 7.27-7.35 (2H, m, Ar-H), 5.59 (1H, s, PhCH-), 5.54 (1H, dd, *J*= 10.4 and 3.2 Hz, H-3), 4.78 (1H, d, *J*= 1.2 Hz, H-1), 4.32 (1H, dd, *J*= 3.2 and 1.2 Hz, H-2), 4.22-4.31 (2H, m, H-5 and H-6a), 3.95-4.03 (1H, m, H-6b), 3.92 (1H, t, *J*= 10.1 Hz, H-4), 3.43 (3H, s, OCH_3).

Methyl 4,6-*O*-benzylidene-2,3-di-*O*-benzoyl-α-D-mannopyranoside (7): The reaction of compound 6 (0.3 g, 0.776 mmol) and benzoyl chloride (0.396 g, 2.817 mmol) in anhydrous pyridine (1 mL) at 0 ^{0}C to room temperature for overnight followed by chromatography (*n*-hexane/ethyl acetate =10/1, v/v) gave the di-*O*-benzoyl derivative, **7** (0.343 g, 90%) as a white crystalline solid. Recrystallization from ethyl acetate/*n*-hexane (1/1, v/v) gave the analytically pure sample as needles, mp 121-122 °C.

R_f = 0.51 (*n*-hexane/ethyl acetate = 4/1, v/v). FT-IR ($CHCl_3$, v, cm^{-1}): 1687, 1682 (CO). ^1H NMR (400 MHz, $CDCl_3$, δ, ppm): 8.12-8.19 (5H, m, Ar-H), 7.57-7.69 (4H, m, Ar-H), 7.41-7.54 (6H, m, Ar-H), 5.81 (1H, dd, *J*= 10.0 and 3.1 Hz, H-3), 5.79 (1H, dd, *J*= 3.1 and 1.2 Hz, H-2), 5.69 (1H, s, PhCH-), 4.93 (1H, d, *J*= 1.2 Hz, H-1), 4.32-4.41 (2H, m, H-5 and H-6a), 4.11-4.19 (1H, m, H-6b), 4.00 (1H, t, *J*= 10.0 Hz, H-4), 3.50 (3H, s, OCH_3).

Antibacterial screening tests

Four Gram-positive bacteria *viz. Bacillus cereus* BTCC 19, *Bacillus megaterium* BTCC 18, *Bacillus subtilis* BTCC 17 and *Staphylococcus aureus* ATCC 6538 and six Gram-negative bacteria *viz*. *Escherichia coli* ATCC 25922, INABAET (vibrio) AE 14748, *Pseudomonas aeruginosa* CRL (ICDDR,B), *Salmonella paratyphi* AE 14613, *Salmonella typhi* AE 14612, and *Shigella dysenteriae* AE 14369 were selected for antibacterial potentiality test. For the detection of antibacterial activities, the disc diffusion method described by Bauer *et al*. [23] was followed. Mueller-Hinton (agar and broth) medium was used for the culture of bacteria. Dimethylformamide (DMF) was initially used as a solvent to prepare the desired solution (1%) of the compounds. The plates were incubated at 37 °C for 48 h. Proper control was maintained with DMF. Each experiment was carried out in triplicate. All the results were compared with the standard antibacterial antibiotic ampicillin [50 µg/disc, Beximco Pharmaceuticals Ltd., Bangladesh].

Results and Discussion

Our main aim was to synthesize 2,3-di-*O*-benzoyl derivatives (**3** and **7**) of methyl α-D-glucopyranoside (**1**) and methyl α-D-mannopyranoside (**4**), respectively, to study and compare their antibacterial properties.

Synthesis of methyl 4,6-*O*-benzylidene-2,3-di-*O*-benzoyl-α-D-glucopyranoside (3)

Initially we prepared methyl 4,6-*O*-benzylidene-α-D-glucopyranoside (**2**) from methyl α-D-glucopyranoside (**1**). The reaction of methyl α-D-glucopyranoside (**1**) with benzaldehyde in the presence of anhydrous zinc chloride for 12 h followed by work-up and chromatography gave a white crystalline solid, mp 162-163 °C (Scheme 1). The FT-IR spectrum of this solid showed bands at 3310-3400 cm^{-1} corresponding to hydroxyl stretching. In its ^1H NMR spectrum, a two-proton multiplet at δ 7.53-7.47, a three-proton multiplet at δ 7.42-7.35 and a one-proton singlet at δ 5.54 clearly indicated the formation of benzylidene acetal in the molecule. This was also confirmed by its ^{13}C NMR spectrum where signals at δ 137.1 (Ar-C), 129.3, 128.3, 126.3 (Ar-CH) and 102.0 (PhCH-) were found for the benzylidene acetal. Complete analysis of its FT-IR, ^1H and ^{13}C NMR spectra led us to assign the structure as methyl 4,6-O-benzylidene-α-D-glucopyranoside (**2**).

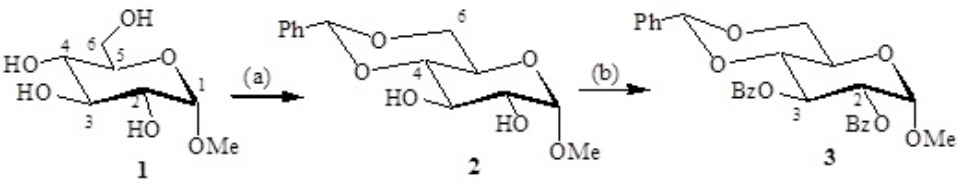

Scheme 1. Reagents and conditions: (a) PhCHO, dry $ZnCl_2$, 25 ^0C, 12 h, 69%. (b) BzCl, dry pyridine, 0 ^0C-RT, 12 h, 92%.

Having protected glucopyranoside **2** in hand, we carried out its dibenzoylation (Scheme 1). Thus, treatment of glucopyranoside **2** with dimolar benzoyl chloride (BzCl) in anhydrous pyridine for 12 h using a catalytic amount of DMAP gave a compound almost in quantitative yield (92%) as needles, mp 146-148 °C. In the FT-IR spectrum of this compound, bands at 1735 and 1719 cm^{-1} were observed for carbonyl frequency and hence indicated the attachment of benzyloxy groups in the molecule. The FT-IR spectrum showed no band for hydroxyl stretching. In the ^1H NMR spectrum, the following peaks were observed in the aromatic region: δ 7.81-8.05 (5H, m), 7.31-7.48 (6H, m) and 7.21-7.30 (4H, m) and a one-proton singlet at δ 5.52 for PhCH-. The more ten aromatic protons in addition to benzylidene acetal protons indicated the attachment of two benzoyloxy groups in the molecule. Also, H-2 (at δ 5.21 as dd) and H-3 (at δ 6.02 as t) protons shifted down field as compared to its precursor compound **2**. This confirmed the attachment of benzoyloxy groups at position C-2 and C-3. So, the structure was established as methyl 4,6-*O*-benzylidene-2,3-di-*O*-benzoyl-α-D-glucopyranoside (**3**).

Synthesis of methyl 4,6-*O*-benzylidene-2,3-di-*O*-benzoyl-α-D-mannopyranoside, 7

Our next attempt was to synthesize methyl 4,6-*O*-benzylidene-2,3-di-*O*-benzoyl-α-D-mannopyranoside, (**7**). For this reason we prepared methyl 3-*O*-benzoyl-α-D-mannopyranoside (**5**) from methyl α-D-mannopyranoside (**4**) by dibutyltin oxide method using literature procedure [8, 24] (Scheme 2).

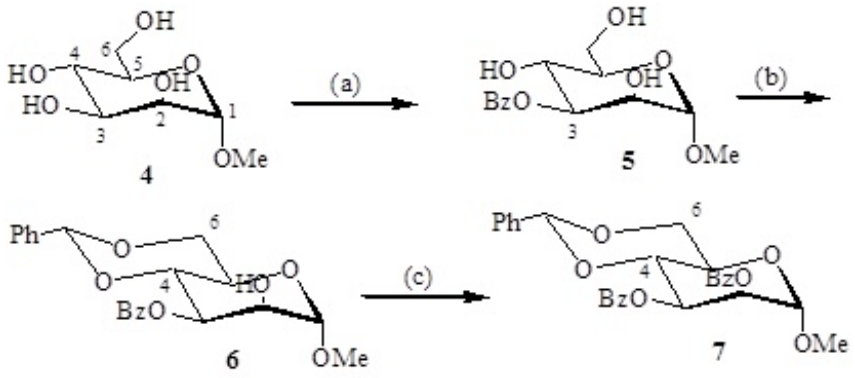

Scheme 2. Reagents and conditions: (a) Bu_2SnO, dry MeOH, reflux, 3h, BzCl, dioxane, RT, 4h, 68%. (b) PhCHO, dry $ZnCl_2$, 25 ^0C, 12 h, 65%. (c) BzCl, 0 ^0C-RT, 12 h, 90%.

In the dibutyltin oxide method initially a stannylene ring (intermediate tin complex) is formed between *cis*-vicinal glycol at C-2 and C-3 position, where the equatorial C-3 OH group is activated without exception (Figure 1). Hence the unimolecular benzoylation occurs at C-3 position only. Thus, the structure of this compound was established as methyl 3-*O*-benzoyl-α-D-mannopyranoside (**5**) by analyzing its FT-IR and ^1H NMR spectra.

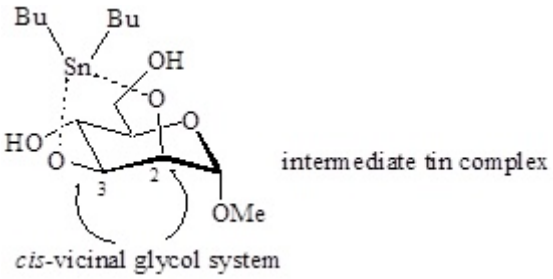

Figure 1. Formation of the intermediate stannylene ring.

The 3-*O*-benzoate **5** was then subjected for 4,6-*O*-benzylidene protection. Thus, the reaction of compound **5** with benzaldehyde in the presence of anhydrous zinc chloride for 12 h followed by work-up and chromatography gave as white needles, mp 135-136 °C. The FT-IR spectrum of this solid showed bands at 3290-3500 (br) and 1735 cm^{-1} corresponding to hydroxyl and carbonyl stretchings, respectively. In its ^1H NMR spectrum, a two-proton doublet at δ 8.05, a one-proton triplet at δ 8.05, a five-proton multiplet at δ 7.39-7.46, a two-proton multiplet at δ 7.27-7.35 and a one-proton singlet at δ 5.59 (PhCH-) clearly indicated the formation of benzylidene acetal and presence of a benzoyl group in the molecule. Complete analysis of its FT-IR and ^1H NMR spectra led us to assign the structure as methyl 3-*O*-benzoyl-4,6-*O*-benzylidene-α-D-mannopyranoside (**6**).

Having protected mannopyranoside **6** in hand, we carried out its 2-*O*-benzoylation. Thus, unimolar benzoylation of **6** with benzoyl chloride in pyridine and chromatography gave a crystalline solid. Recrystallization from ethyl acetate/*n*-hexane (1:1, v:v) gave the analytically pure sample as needles, mp 121-122 °C (Scheme 2). The FT-IR spectrum showed no band for hydroxyl stretching. In the FT-IR spectrum of this compound, bands at 1687 and 1682 cm^{-1} were observed for carbonyl frequency. In the ^1H NMR spectrum of this compound the following peaks were observed in the aromatic region: δ 8.12-8.19 (5H, m), 7.57-7.69 (4H, m), 7.41-7.54 (6H, m) and a one-proton singlet at δ 5.69 (PhCH-). The additional five aromatic protons than that of 3-*O*-benzoate **6** indicated the attachment of one more benzoyloxy groups in the molecule. Also, H-2 (at δ 5.79 as dd) protons shifted down field as compared to its precursor compound **6**. Thus, the structure of the compound was assigned as methyl 4,6-O-benzylidene-2,3-di-O-benzoyl-α-D-mannopyranoside (**7**).

Antibacterial activities of the synthesized compounds

The results of the *in vitro* inhibition zone against the selected Gram-positive bacteria due to the effect of the chemicals (**1-7**) are mentioned in Table 1. It was observed from Table 1 that the tested chemicals were less effective against these Gram-positive organisms. Only methyl 4,6-*O*-benzylidene-2,3-di-*O*-benzoyl-α-D-mannopyranoside (**7**) exhibited considerable inhibition (*20 mm) against *Bacillus cereus* which was comparable to that of the standard antibiotic, ampicillin (*22 mm).

Table 1. Inhibition against Gram-positive organisms by the tested chemicals (**1-7**).

Compound no.	Diameter of zone of inhibition, in mm (50 µg, dw / disc)			
	Bacillus cereus	*Bacillus megaterium*	*Bacillus subtilis*	*Staphylococcus aureus*
1	N/A	N/A	N/A	N/A
2	08	N/A	N/A	N/A
3	08	N/A	N/A	N/A
4	N/A	N/A	N/A	N/A
5	08	N/A	11	N/A
6	N/A	N/A	N/A	N/A
7	*20	N/A	N/A	N/A
****Ampicillin**	*22	19	*25	*21

NB. "N/A" indicates no inhibition, dw = dry weight, "**" indicates standard antibiotic, "*" shows good inhibition.

Inhibition zone against the selected Gram-negative bacteria due to the effect of the monosaccharides (**1-7**) are mentioned in Table 2. The test chemicals showed better activity against these organisms as compared to that of Gram-positive organisms. The compounds (**1-7**) did not show considerable inhibition against *E. coli* and INABAET (vibrio). The study revealed that the tested chemicals were more effective against *Salmonella paratyphi* and *Salmonella typhi*.

Table 2. Inhibition of the tested chemicals **(1-7)** against Gram-negative organisms.

	Diameter of zone of inhibition in mm (50 µg dw / disc)					
Compound no	*E. coli*	INABAET (vibrio)	*Pseudomonas aeruginosa*	Salmonella paratyphi	*Salmonella typhi*	*Shigella dysenteriae*
1	N/A	N/A	N/A	08	N/A	N/A
2	N/A	07	N/A	06	07	N/A
3	06	12	08	09	14	N/A
4	N/A	N/A	N/A	*21	*20	N/A
5	08	N/A	14	*20	*20	N/A
6	N/A	09	12	*21	*22	N/A
7	15	N/A	14	17	18	13
****Ampicillin**	*25	*24	17	*35	13	*35

NB. N/A indicates no zone of inhibition. dw= dry weight. ** indicates standard antibiotic, * shows good inhibition.

Structure activity relationship (SAR)

In vitro antibacterial study revealed that the monosaccharide derivatives (**1-7**) were more active against some Gram-negative organisms than that of Gram-positive organisms. An important observation was that the benzoylated mannopyranosides (**5-7**) were more active than that of the glucopyranosides (**2-3**). Again, compounds **1**, **2** and **4** showed poor toxicity than that of compounds **3**, **6**, and **7** against these pathogens. This is probably due to the presence of more hydroxyl groups in **1**, **2** and **4**. While compounds **3**, **6** and **7** having fewer or no hydroxyl groups showed much better antibacterial potentiality (mannopyranoside **5** was found to be exceptional). Here the hydrophobicity of the molecules increased gradually from compounds **1**, **2**, and **4** to **3**, **6**, and **7**. The hydrophobicity of compounds is an important parameter for bioactivity and is directly related to membrane permeation [25]. We believe that similar hydrophobic interaction might occur between the benzoyl groups of monosaccharides (**3** and **7**) accumulated in the lipid membranes of bacteria. As a consequence of their hydrophobic interaction, bacteria lose their membrane permeability [26], ultimately causing death of the bacteria.

Conclusion

We have synthesized methyl 4,6-*O*-benzylidene-2,3-di-*O*-benzoyl-α-D-glucopyranoside (**3**) and methyl 4,6-*O*-benzylidene-2,3-di-*O*-benzoyl-α-D-mannopyranoside (**7**) from methyl α-D-glucopyranoside (**1**) and methyl α-D-mannopyranoside (**4**), respectively in reasonably good yields. A comparative *in vitro* antibacterial study of these compounds was carried out successfully employing ten bacterial pathogens. The structure activity relationship (SAR) study revealed that the benzoylated mannopyranosides (**5-7**) were more active against the tested organisms than that of the glucopyranosides (**1-3**).

Acknowledgments

We are grateful to the Research Cell, University of Chittagong for research grant (Sl. no. 83/07, 2014) to carry out the research work. We would like to thank Dr. M.S. Rahman, Department of Microbiology, University of Chittagong, for the antibacterial tests of the synthesized compounds.

References

[1] Schaffer R. The Carbohydrates: Chemistry and Biochemistry. Pigman W, Horton D. (eds.), 2nd ed: Academic Press: New York; 1972. ISBN: 978-0318502380.

[2] Kochetkov NK, Dmitrive BA, Backinowsky LV. New sugars from antigenic lipopolysaccharides of bacteria: identification and synthesis of 3-*O*-[(*R*)-1-carboxyethyl]-L-rhamnose, an acidic component of *Shigella dysenteriae* type 5 lipopolysaccharide. Carbohydrate Research 1976;51/2:229-237. DOI: 10.1016/S0008-6215(00)83330-3.

[3] Dhavale DD, Matin MM. Selective sulfonylation of 4-*C*-hydroxymethyl-β-L-threo-pento-1,4-furanose: synthesis of bicyclic diazasugars. Tetrahedron 2004;60/19,4275-4281. DOI: 10.1016/j.tet.2004.03.034.

[4] Dhavale DD, Matin MM. Piperidine homoazasugars: natural occurrence, synthetic aspects and biological activity study. Arkivoc 2005;iii:110-132. url: http://www.arkat-usa.org/get-file/18916/

[5] Matin MM, Bhuiyan MMH, Azad AKMS, Bhattacharjee SC, Harun-Or-Rashid M. Synthesis and antimicrobial studies of 6-*O*-lauroyl-1,2-*O*-isopropylidene-α-D-gluco-furanose derivatives. Chemistry & Biology Interface 2014;4/4:223-231. url: http://www.cbijournal.com/paper-archive/july-august-2014-vol-4/

[6] Matin MM, Bhuiyan MMH, Debnath DC, Manchur MA. Synthesis and comparative antimicrobial studies of some acylated D-glucofuranose and D-glucopyranose derivatives. International Journal Biosciences 2013;3/8:279-287. DOI: 10.12692/ijb/3.8.279-287.

[7] Matin MM. Synthesis and antimicrobial study of some methyl 4-*O*-palmitoyl-α-L-rhamnopyranoside derivatives. Orbital: The Electronic Journal of Chemistry 2014;6/1:20-28. url: http://www.orbital.ufms.br/index.php/Chemistry/article/view/553/pdf

[8] Tusda Y, Haque ME, Yosimoto K. Regioselective monoacylation of some glycopyranosides via cyclic tin intermediates. Chemical and Pharmaceutical Bulletin 1983;31/5:1612-1624. DOI: 10.1248/cpb.31.1612.

[9] Kabir AKMS, Matin MM, Ali M, Anwar MN. Comparative studies on selective acylation and antimicrobial activities of some D-glucofuranose derivatives. Journal of Bangladesh Academy of Sciences 2003;27/1):43-50. url: https://www.researchgate.net/publication/272747199.

[10] Kabir AKMS, Matin MM, Bhuiyan MMR, Rahim MA. Synthesis and characterization of some acylated derivatives of D-mannose. The Chittagong University Journal of Science 2001;25/1:65-73. url: https://www.researchgate.net/publication/272791894.

[11] Kobayashi T. Lipase-catalyzed syntheses of sugar esters in non-aqueous media. Biotechnology Letters 2011;33/10:1911-1919. DOI: 10.1007/s10529-011-0663-z.

[12] Microwave in Organic Synthesis. Loupy A. (ed), 2nd ed: Wiley-VCH Verlag GmbH & Co.: Weinheim; 2006. ISBN: 3-527-31452-0.

[13] Perez-Tomas R. Multidrug resistance: retrospect and prospects in anti-cancer drug treatment. Current Medicinal Chemistry 2006;13/16:1859-1876. DOI: 10.2174/092986706777585077.

[14] Ahsan F, Arnold JJ, Meezan E, Pillion DJ. Sucrose cocoate, a component of cosmetic preparations, enhances nasal and ocular peptide absorption. International Journal of Pharmaceutics 2003;251:195-203. DOI: 10.1016/S0378-5173(02)00597-5.

[15] Csóka G, Marton S, Zelko R, Otomo N, Antal I. Application of sucrose fatty acid esters in transdermal therapeutic systems. European Journal of Pharmaceutics & Biopharmaceutics 2007, 65/2, 233-237. DOI: 10.1016/j.ejpb.2006.07.009.

[16] Pouillart P, Douillet O, Scappini B, Gozzini A, Santini V, Grossi A, et al. Regioselective synthesis and biological profiling of butyric and phenylalkylcarboxylic esters derivated from D-mannose and xylitol: influence of alkyl chain length on acute toxicity. European Journal of Pharmaceutical Sciences 1999;7/2:93-106. DOI: 10.1016/S0928-0987(98)00011-6.

[17] Chortyk OT, Pomonis JG, Johnson AW. Synthesis and characterizations of some insecticidal sucrose esters. Journal of Agricultural & Food Chemistry, 1996;44/6:1551-1557. DOI: 10.1021/jf950615t.

[18] Kabir AKMS, Matin MM, Sanaullah AFM, Sattar MA, Rahman MS. Antimicrobial activities of some lyxoside derivatives. Bangladesh Journal of Microbiology 2001;18/1:89-95. url: https://www.researchgate.net/publication/272677730.

[19] Kabir AKMS, Matin MM, Bhuiyan MMR, Rahim MA, Rahman MS. Biological evaluation of some monosaccharide derivatives. International Journal of Agriculture & Biology 2005;7/2: 218-221. DOI: 1560–8530/2005/07–2–218–221.

[20] Kabir AKMS, Matin MM, Mridha MAU, Shahed SM. Antifungal activities of some methyl 6-O-trityl-α-D-mannopyranosides. The Chittagong University Journal of Science 1998;22/1:41-46. url: https://www.researchgate.net/publication/272833648.

[21] Kabir AKMS, Matin MM, Rahman MS. Antimicrobial activities of some rhamnoside derivatives. Chittagong University Journal of Science 2000;24/1:129-135. url: https://www.researchgate.net/publication/272792469.

[22] Demchenko AV, Pornsuriyasak P, de Meo C. Acetal protecting groups in the organic laboratory: Synthesis of methyl 4,6-O-benzylidene-α-D-glucopyranoside. Journal of Chemical Education 2006;83/5:782-784. DOI: 10.1021/ed083p782.

[23] Bauer AW, Kirby WMM, Sherris JC, Turck M. Antibiotic susceptibility testing by a standardized single disk method. American Journal of Clinical Pathology 1966;45/4: 493-496. Pubmed: http://www.ncbi.nlm.nih.gov/pubmed/5325707.

[24] Nashed MA, Anderson L. Organotin derivatives and the selective acylation and alkylation of the equatorial hydroxy group in a vicinal, equatorial-axial pair. Tetrahedron Letters 1976;17/39:3503-3506. DOI: 10.1016/S0040-4039(00)71342-6.

[25] Kim YM, Farrah S, Baney RH. Structure-antimicrobial activity relationship for silanols, a new class of disinfectants, compared with alcohols and phenols. International Journal of Antimicrobial Agents 2007;29/2:217-222. DOI: org/10.1016/j.ijantimicag.2006.08.036.

[26] Judge V, Narasimhan B, Ahuja M, Sriram D, Yogeeswari P, Clercq ED, Pannecouque C, Balzarini J. Synthesis, antimycobacterial, antiviral, antimicrobial activity and QSAR studies of N2-acyl isonicotinic acid hydrazide derivatives. Medicinal Chemistry 2013;9/1:53-76. DOI: 10.2174/157340613804488404.

JOTCSA, volume 2, issue 4 (2015), pp. 22-31

Research Article

http://dergipark.ulakbim.gov.tr/jotcsa

Synthesis and antioxidant activity of some novel derivatives of bis-2-azetidinones and bis-4-thiazolidinones

Avinash Shinde[a]*, Sainath Zangade[b], Shivaji Chavan[b], and Sachin Tiwde[a]

[a]P.G.Department of Chemistry, N.E.S.Science College, Nanded-431605 (M.S.), India.
[b] P.G.Department of Chemistry, Y.M.Nanded-431602 (M.S.), India
E-mail: dr.atshinde@gmail.com Tel.: +919423534248; fax: +91.246.2250465

Abstract: In present study, several bis- 2-azetidinones **2a-g** and bis-4-thiazolidinones **3a-g** have been synthesized from ethylenediaminebis-Schiff bases using conventional as well as microwave techniques. The newly synthesized compounds were established on the basis of spectroscopic techniques. Further, all compounds were screened for antioxidant activity; most of the titled compounds show potent activity.

Submitted: February 10, 2015. **Revised:** April 11, 2015. **Accepted:** April 12, 2015.

Keywords: Bis-Schiff bases, bis-2-azetidinones, bis-4-thiazolidinones, microwave technique, antioxidant activity.

Introduction

Literature survey reveals that most of the compounds having thiazolidiones and azetidinones nuclei possess pharmacological activity [1, 2]. Azetidinones which are part of antibiotic structures are known to exhibit interesting biological activities. A large number of 3-chloro monocyclic β-lactams possesses powerful antibacterial, antimicrobial, anti-inflammatory, anticonvulsant and antitubercular activities [3-5]. They also function as enzyme inhibitors and are effective on the central nervous system [6-8]. 4-Thiazolidinones and its derivatives are known to possess a verity of physiological viz. analgesic local [9] and spiral [10] antimicrobial [11], hypnotics [12], antibacterial [13], antifungal [14], antitubercular [15], anticancer and anti-HIV [16].

The classical synthesis of these compounds involves cycloaddition of monochloroacetyl chloride with imine (Schiff base) resulting in the formation of 2-azetidinone (β-lactam) [17]. Conventional synthesis of 4-thiazolidinones involves the cyclocondensation between the Schiff base and mercaptoacetic acid [18, 19]. As part of our interest towards the development of novel heterocycles [20-24], herein we wish to report the synthesis of bis-2-azetidinones 2a-g and bis-4-thiazolidinones 3a-g by the reaction of bis-imines 1a-g with chloroacetyl chloride and thioglycolic acid, respectively, using conventional as well as microwave technique (Scheme 1).

Materials and Methods

Chemicals and Apparatus

Melting points were determined in an open capillary tube and are uncorrected. FT-IR spectra were recorded in KBr on a Perkin-Elmer spectrometer. 1H NMR spectra were recorded on a Gemini 300-MHz instrument in DMSO as solvent and TMS as an internal standard. The mass spectra were recorded on EI-Shimadzu-GC-MS spectrometer. Elemental analyses were performed on a Perkin-Elmer 240 CHN elemental analyzer. Synthos-3000, Anton Paar reaction system was used for microwave synthesis.

Synthesis of bis-Schiff bases (1a-g)

Compounds **1a-g** were synthesized according to given method in literature [31]. 1,2-ethylenediamine (0.001 mole) and aldehyde (0.002 mole) were dissolved in ethanol (15 mL), acetic acid (0.2 mL) was added, and the reaction mixture was refluxed for 2-15 min. Reaction was monitored on TLC. Half of the solvent was evaporated and the rest was cooled. The separated solid was filtered, washed with water, and crystallized from ethanol.

General procedure for preparation of bis-2-azetidinones (2a-g); conventional technique

Synthesis of 1,1-ethane-1,2-diylbis(3-chloro-4(3-ethoxy-4-hydroxy-5-iodophenyl)azetidin-2-one (**2c**)

A solution of bis (3-ethoxy-4-hydroxy-5-iodophenyl)benzylidene-1,2-ethylenediamine (0.001 mole, 0.463 mg) in dry dioxane (15 mL) was added to well stirred mixture of chloroacetyl chloride (0.004 mole) and triethyl amine (0.006 mole) in dry 1,4-dioxane at 0^0C. The reaction mixture was stirred for 6 hrs. Excess of solvent was distilled and the resultant solid was poured into ice–cold water. The separated solid was filtered and recrystallized from alcohol to give 2c.

Microwave technique

Synthesis of 1,1-ethane-1,2-diylbis(3-chloro-4(3-ethoxy-4-hydroxy-5-iodophenyl)azetidin-2-one. (2c)

A mixture of bis(3-ethoxy-4-hydroxy-5-iodophenyl)benzylidene-1,2-ethylenediamine (0.001 mole, 0.463 mg) in dry dioxane (15 mL) was taken in conical flask, and chloroacetyl chloride (0.004 mole) and triethyl amine (0.006 mole) were added slowly at 0-5 ^{0}C. Then the reaction mixture was transferred to microwave reaction vessel equipped with a magnetic stirrer (Synthos-3000). The vessel was sealed and the reaction mixture was irraditated by 50 W intermittently at 30 sec. interval for 5 min. The solid so formed was recrystallized from ethyl alcohol to give **2c**. Some of the physical data of the synthesized compounds **2a-g** are given in Table 1.

1,1-Ethane-1,2-diylbis(3-chloro-4(3-ethoxy-4-hydroxyphenyl)azetidin-2-one) (2a)

FT-IR (KBr cm^{-1}): 3480 (Ar-OH stretching), 1670 (C=O stretching), 1470, 1450 (Aromatic C=C stretching), 1380 (C-N stretching). ^{1}H NMR (300 MHz, DMSO-d_6, δ, ppm): 1.35 (t, 6H, -2CH_3), 2.80 (s, 2H, -2CH), 3.68 (s, 4H, -2NCH_2), 4.15 (q, 4H, -2OCH_2), 5.06 (s,2H,-2CH-Cl), 6.32-7.51 (m, 6H, -2ArH), 13.2(s,2H,-2Ar-OH). MS (m/z): 509(M+). Anal. calcd. for $C_{24}H_{26}Cl_2N_2O_6$: C,56.58; H, 5.10. Found: C, 55.28; H, 5.35.

1,1-Ethane-1,2-diylbis(3-chloro-4(3-ethoxy-4-hydroxy-5-bromophenyl)azetidin-2-one) (2b)

FT-IR (KBr cm^{-1}): 3435 (Ar-OH stretching), 1685 (C=O stretching), 1455, 1440 (Aromatic C=C stretching), 1380, 1385 (C-N stretching). ^{1}H NMR (300 MHz, DMSO-d_6, δ, ppm): 1.38 (t, 6H, -2CH_3), 2.85 (s, 2H, -2CH), 3.70 (s, 4H, -2NCH_2), 4.01 (q, 4H, -2OCH_2), 5.12 (s,2H,-2CH-Cl), 6.53-7.80 (m, 4H, -2ArH), 13.01(s,2H,-2Ar-OH). MS (m/z): 667 (M+). Anal. calcd. for $C_{24}H_{24}$ Br_2Cl_2 N_2O_6: C,43.76; H, 3.90. Found: C,43.28; H, 3.35.

1,1-Ethane-1,2-diylbis(3-chloro-4(3-ethoxy-4-hydroxy-5-iodophenyl)azetidin-2-one) (2c)

FT-IR (KBr cm^{-1}): 3410 (Ar-OH stretching), 1690 (C=O stretching), 1440, 1425 (Aromatic C=C stretching), 1370 (C-N stretching). ^1H NMR (300 MHz, DMSO-d_6, δ, ppm): 1.35 (t, 6H, -2CH_3), 2.83 (s, 2H, -2CH), 3.65 (s, 4H, -2NCH_2), 4.15 (q, 4H, -2OCH_2), 5.16 (s,2H,-2CH-Cl), 6.65-7.85 (m, 4H, -2ArH), 13.10 (s, 2H,-2Ar-OH). MS (m/z): 761 (M+). Anal. calcd. for $C_{24}H_{24}Cl_2I_2N_2O_6$: C,37.56; H, 3.15. Found: C,37.28; H, 3.35.

1,1-Ethane-1,2-diylbis(3-chloro-4(3-methox-4-hydroxyphenyl)azetidin-2-one) (2d)

FT-IR (KBr cm^{-1}): 3425 (Ar-OH stretching), 1678 (C=O stretching), 1460, 1444 (Aromatic C=C stretching), 1378 (C-N stretching). ^1H NMR (300 MHz, DMSO-d_6, δ, ppm): 2.82 (s, 2H, -2CH), 3.40 (s, 4H, -2NCH_2), 3.75 (s, 6H, -2OCH_3), 5.01 (s,2H,-2CH-Cl), 6.25-7.30 (m, 6H, -2ArH), 13.60 (s,2H,-2Ar-OH). MS (m/z): 483 (M+). Anal. calcd. for $C_{22}H_{24}Cl_2N_2O_6$: C,54.56; H, 4.96 Found: C,54.80; H, 4.30.

1,1-Ethane-1,2-diylbis(3-chloro-4(3-methoxy-4-hydroxy-5-bromophenyl)azetidin-2-one) (2e)

FT-IR (KBr cm^{-1}): 3445 (Ar-OH stretching), 1682 (C=O stretching), 1465, 1450 (Aromatic C=C stretching), 1380 (C-N stretching). ^1H NMR (300 MHz, DMSO-d_6, δ, ppm): 2.83 (s, 2H, -2CH), 3.43 (s, 4H, -2NCH_2), 3.78 (s, 6H, -2OCH_3), 5.12 (s, 2H,-2CH-Cl), 6.30-7.35 (m, 4H, -2ArH), 13.40 (s, 2H,-2Ar-OH). MS (m/z): 613 (M+). Anal. calcd. for $C_{22}H_{22}Br_2Cl_2\ N_2O_6$: C,43.06; H, 3.58. Found: C, 43.80; H, 3.30.

1,1-Ethane-1,2-diylbis(3-chloro-4(3-methoxy-4-hydroxy-5-chlorophenyl)azetidin-2-one) (2f)

FT-IR (KBr cm^{-1}): 3480(Ar-OH stretching), 1688 (C=O stretching), 1475, 1455 (Aromatic C=C stretching), 1385 (C-N stretching). ^1H NMR (300 MHz, DMSO-d_6, δ, ppm): 2.86 (s, 2H, -2CH), 3.47 (s, 4H, -2NCH_2), 3.80 (s, 6H, -2OCH_3), 5.20 (s,2H,-2CH-Cl), 6.42-7.40 (m, 4H, -2ArH), 13.32 (s,2H,-2Ar-OH). MS (m/z): 556 (M+). Anal. calcd. for $C_{22}H_{22}Cl_4N_2O_6$: C,47.48; H, 3.95. Found: C, 47.76; H, 4.00.

1,1-Ethane-1,2-diylbis(3-chloro-4(3-methoxy-4-hydroxy-5-iodophenyl)azetidin-2-one) (2g)

FT-IR (KBr cm^{-1}): 3428 (Ar-OH stretching), 1681 (C=O stretching), 1460, 1445 (Aromatic C=C stretching), 1382 (C-N stretching). ^1H NMR (300 MHz, DMSO-d_6, δ, ppm): 2.85 (s, 2H, -2CH), 3.42 (s, 4H, -2NCH_2), 3.69 (s, 6H, -2OCH_3), 5.15 (s,2H,-2CH-Cl), 6.35-7.25 (m, 4H, -2ArH), 13.10 (s,2H,-2Ar-OH). MS (m/z): 640 (M+). Anal. calcd. for $C_{22}H_{22}Cl_2I_2N_2O_6$: C,41.25; H, 3.43. Found: C,41.80; H, 3.56.

General procedure for preparation of bis-4-thiazolidinone

Conventional synthesis of 3,3-ethane-1,2-diylbis(2-(3-ethoxy-4-hydroxy-5-iodophenyl)-1,3-thiazolidin-4-one) (3c)

A mixture of bis(3-ethoxy-4-hydroxy-5-iodophenyl)benzylidene-1,2-ethylenediamine (0.001 mole, 0.462 mg) in 1,4-dioxane (15 mL) containing anhydrous $ZnCl_2$ (0.02 g) and thioglycolic acid (0.002 mole) was refluxed for 8 hrs. The reaction mixture was cooled and poured into ice cold water. The separated solid was filtered and recrystallized from 1,4-dioxane to give **3c**.

Microwave technique

Synthesis of 3,3-ethane-1,2-diylbis(2-(3-ethoxy-4-hydroxy-5-iodophenyl)-1,3-thiazolidin-4-one).(3c)

A homogeneous mixture of bis(3-ethoxy-4-hydroxy-5-iodophenyl)benzylidene-1,2-ethylenediamine (0.001 mole, 0.462 mg) in 1,4-dioxane (15 mL) containing anhydrous $ZnCl_2$ (0.02 g) and thioglycolic acid (0.002 mole) was introduced to a microwave reaction vessel equipped with a magnetic stirrer (Synthos-3000). The vessel was sealed and the reaction was irradiated by 50 W intermittently at 30 sec. interval for 5 min. The solid formed was filtered and recrystallized from ethyl alcohol to give **3c**. Some of the physical data of synthesized compounds **3a-g** are given in Table 2.

3,3-Ethane-1,2-diylbis(2-(3-ethoxy-4-hydroxyphenyl)-1,3-thiazolidin-4-one(3a)

FT-IR (KBr cm^{-1}): 3525 (Ar-OH stretching), 1792 (C=O stretching), 1570, 1530,1440 (Aromatic C=C stretching). ^1H NMR (300 MHz, DMSO-d_6, δ, ppm): 1.30 (t, 6H, -2CH_3), 3.29 (s, 2H, -2CH), 4.19 (q, 4H, -2OCH_3), 5.10 (s,4H,-2CH_2-S), 7.20-7.95 (m, 6H, -2ArH), 13.01(s, 2H, -2Ar-OH). MS (m/z): 504 (M^+). Anal. calcd. for $C_{24}H_{28}N_2O_6S_2$: C,57.24; H, 5.50. Found: C,57.80; H, 5.56.

3,3-Ethane-1,2-diylbis(2-(3-ethoxy-4-hydroxy-5-bromophenyl)-1,3-thiazolidin-4-one(3b)

FT-IR (KBr cm^{-1}): 3535 (Ar-OH stretching), 1795 (C=O stretching), 1575, 1540,1450 (Aromatic C=C stretching). ^1H NMR (300 MHz, DMSO-d_6, δ, ppm): 1.36 (t, 6H, -2CH_3), 3.32 (s, 2H, -2CH), 4.21 (q, 4H, -2OCH_3), 5.16 (s,4H,-2CH_2-S), 7.30-7.85 (m, 4H, -2ArH), 13.0 (s,2H,-2Ar-OH). MS (m/z): 662 (M^+). Anal. calcd. for $C_{24}H_{26}Br_2N_2O_6S_2$: C,43.50; H, 3.92. Found: C,43.70; H, 3.96.

3,3-Ethane-1,2-diylbis(2-(3-ethoxy-4-hydroxy-5-iodophenyl)-1,3-thiazolidin-4-one (3c)

FT-IR (KBr cm^{-1}): 3530(Ar-OH stretching), 1790 (C=O stretching), 1555, 1530,1450 (Aromatic C=C stretching). ^1H NMR (300 MHz, DMSO-d_6, δ, ppm): 1.28 (t, 6H, -2CH_3), 3.29 (s, 2H, -2CH), 4.18 (q, 4H, -2OCH_3), 4.96 (s,4H,-2CH_2-S), 7.35-7.75 (m, 4H, -2ArH), 13.05 (s, 2H, -2Ar-OH). MS (m/z): 756 (M^+). Anal. calcd. for $C_{24}H_{26}I_2N_2O_6S_2$: C, 38.09; H, 3.43. Found: C,38.26; H, 3.56.

3,3-Ethane-1,2-diylbis(2-(3-methoxy-4-hydroxyphenyl)-1,3-thiazolidin-4-one(3d)

FT-IR (KBr cm^{-1}): 3525 (Ar-OH stretching), 1788 (C=O stretching), 1553, 1540,1435 (Aromatic C=C stretching). ^1H NMR (300 MHz, DMSO-d_6, δ, ppm): 3.30 (s, 2H, -2CH), 3.50 (s, 4H, -2NCH_2), 3.70 (s, 6H, -2OCH_3), 4.86 (s,4H,-2CH_2-S), 7.38-7.80 (m, 6H, -2ArH), 12.05 (s,2H,-2Ar-OH). MS (m/z): 476 (M^+). Anal. calcd. for $C_{22}H_{24}N_2O_6S_2$: C,55.46; H, 5.04. Found: C,54.50; H, 5.25.

3,3-Ethane-1,2-diylbis(2-(3-methoxy-4-hydroxy-5-bromophenyl)-1,3-thiazolidin-4-one(3e)

FT-IR (KBr cm^{-1}): 3540 (Ar-OH stretching), 1793 (C=O stretching), 1558, 1545,1440 (Aromatic C=C stretching). ^1H NMR (300 MHz, DMSO-d_6, δ, ppm): 3.32 (s, 2H, -2CH), 3.53 (s, 4H, -2NCH_2), 3.73 (s, 6H, -2OCH_3), 4.88 (s,4H,-2CH_2-S), 7.40-7.85 (m, 4H, -2ArH), 12.14 (s, 2H, -2Ar-OH). MS (m/z): 634 (M^+). Anal. calcd. for $C_{22}H_{22}Br_2N_2O_6S_2$: C, 41.64; H, 3.47. Found: C,41.30; H, 3.80.

3,3-Ethane-1,2-diylbis(2-(3-methoxy-4-hydroxy-5-chlorophenyl)-1,3-thiazolidin-4-one(3f)

FT-IR (KBr cm^{-1}): 3550 (Ar-OH stretching), 1794 (C=O stretching), 1568, 1555, 1450 (Aromatic C=C stretching). ^1H NMR (300 MHz, DMSO-d_6, δ, ppm): 3.35 (s, 2H, -2CH), 3.56 (s, 4H, -2NCH_2), 3.78 (s, 6H, -2OCH_3), 4.89 (s,4H,-2CH_2-S), 7.43-7.85 (m, 4H, -2ArH), 13.14 (s, 2H, -2Ar-OH). MS (m/z): 546 (M^+). Anal. calcd. for $C_{22}H_{22}Cl_2N_2O_6S_2$: C, 48.35; H, 4.09. Found: C, 48.20; H, 4.20.

3,3-Ethane-1,2-diylbis(2-(3-methoxy-4-hydroxy-5-iodophenyl)-1,3-thiazolidin-4-one(3g)

FT-IR (KBr cm^{-1}): 3520 (Ar-OH stretching), 1790 (C=O stretching), 1550, 1530,1452 (Aromatic C=C stretching). ^1H NMR (300 MHz, DMSO-d_6, δ, ppm): 3.27 (s, 2H, -2CH), 3.41 (s, 4H, -2NCH_2), 3.69(s, 6H, -2OCH_3), 4.81 (s,4H,-2CH_2-S), 7.31-7.75 (m, 4H, -2ArH), 13.01 (s, 2H, -2Ar-OH). MS (m/z): 728 (M^+). Anal. calcd. for $C_{22}H_{22}I_2N_2O_6S_2$: C,36.26; H, 3.02. Found: C, 36.40; H, 4.30.

Antioxidative activity

The following antioxidative methods were used to evaluate the antioxidative properties of our test compounds.

DPPH• Scavenging Activity

DPPH is a stable free radical that can accept an electron or hydrogen radical to become a stable diamagnetic molecule. Due to its odd electron, the methanolic solution of DPPH shows a strong absorption band at 517 nm. DPPH radical reacts with various electron donating molecules (reducing agents or antioxidants). When electrons become paired off, the result is that DPPH solution is bleached. This results in the formation of the colorless 2,2'-diphenyl-1-picryl hydrazine. Reduction of the DPPH radicals can be estimated quantitatively by measuring the decrease in absorbance at 517 nm.

Procedure: Equal volumes of 100 µM 2,2'-diphenyl-1-picrylhydrazyl (DPPH) in methanol was added to different concentrations of test compounds (0 – 200 µM/mL) in methanol, mixed well and kept in dark for 20 min. The absorbance at 517 nm was measured using the Shimadzu UV-1650 spectrophotometer. Plotting the percentage DPPH• scavenging against concentration gave the standard curve and the percentage scavenging was calculated from the following equation:

$$\%\text{scavenging} = \frac{\text{Absorbance of blank} - \text{Absorbance of test}}{\text{Absorbance of blank}} \times 100$$

IC50 was obtained from a plot between concentration of test compounds and % scavenging. Ascorbic acid was used as standard for comparison.

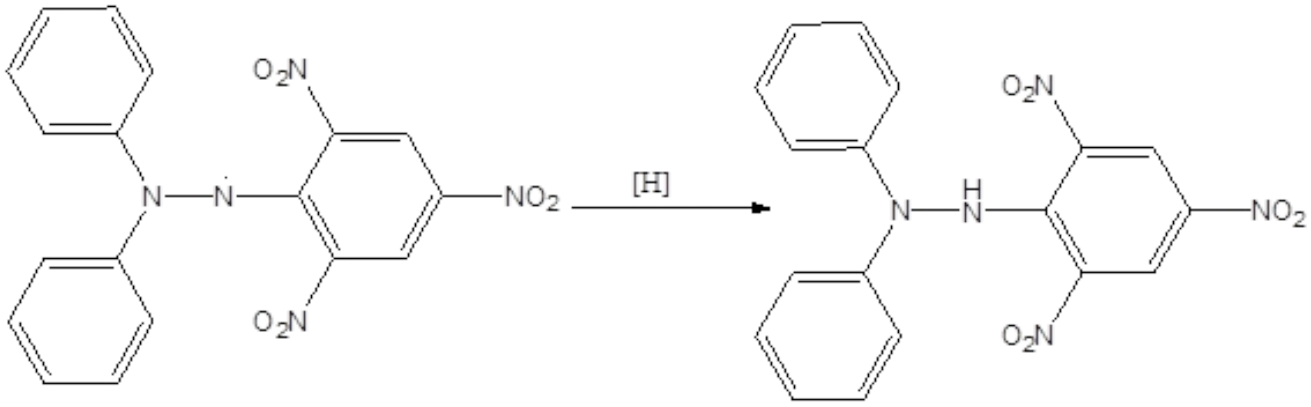

Structural changes occur with DPPH during oxidation

Nitric Oxide Scavenging Activity

Nitric oxide (NO) will be generated by sodium nitroprusside in solution. In the presence of an antioxidant or nitric oxide scavenger, the amount of NO generated will be less. The excess NO will be estimated by Griess reagent, which is the mixture of sulfanilic acid and naphthylethylenediamine dihydrochloride. The nitric oxide will give pink colored complex estimated at 540 nm.

Procedure: To a reaction mixture (6 mL) containing sodium nitroprusside (10 mM, 4 mL), phosphate buffer saline (PBS, 1.0 mL) and 1.0 mL of different concentration of test compounds/standard were incubated at 25ºC for 150 min. After incubation, 0.5 mL of the reaction mixture containing nitrate was removed and 1.0 mL of sulfanilic acid was added, mixed well and allowed to stand for 5 min for completion of diazotization. Then 1.0 mL of naphthylethylenediamine dihydrochloride was added, mixed and allowed to stand for 30 min in dark at room temperature.

The absorbance of these solutions was measured at 540 nm against corresponding blank solution without sodium nitroprusside [29-30]. The % scavenging and IC50 values were determined as explained in DPPH assay.

Results and discussion

In view of the importance of this class of heterocycles and in continuation of our earlier investigations, we have reported the synthesis of 4-thiazolidinones from imines and some of the thiazolidinones were found to have antibacterial action [25]. Therefore, in the present paper, we synthesized a new class of bis- 2-azetidinones and bis-4-thiazolidinones by cyclocondensation reaction of imines 1a-g (Scheme 1). The halo-substituted hydroxybenzaldehydes required for the preparation of imines were prepared by iodination of substituted hydroxybenzaldehydes using molecular iodine and iodic acid by refluxing technique [26]. The 1a-g on cyclocondensation with chloroacetyl chloride afford bis-2-azetidinones 2a-g and with thioglycolic acid afford bis-4-thiazolidinones 3a-g using both conventional as well as MWI techniques. MWI technique were used over conventional technique due to the application of microwave (MW) irradiation as a non-conventional energy source for activation of reactions has now become a very popular and useful technology in organic chemistry [27]. Many researchers have described accelerated organic reactions towards proving the synthetic utility of MW irradiation in routine organic synthesis [28]. Thus, MW techniques has many advantages including easy work-up procedure, short reaction time, and does not need any effort for isolation of products giving high percentage yields. The structures of newly synthesized compounds 2a-g & 3a-g respectively, have been confirmed by elemental analysis, FT-IR, NMR and MS spectral studies. In 1H NMR spectra of bis-2-azetidinones obtained at δ value 2.85 and δ near 5.0 is due to proton of CH-N and CH-Cl respectively. The 1H NMR spectra of bis-4-thiazolidinones show characteristics δ value at 4.90 due to two protons of –CH2S. The δ value at 3.32 is due to –CH of five-membered thiazolidinone ring.

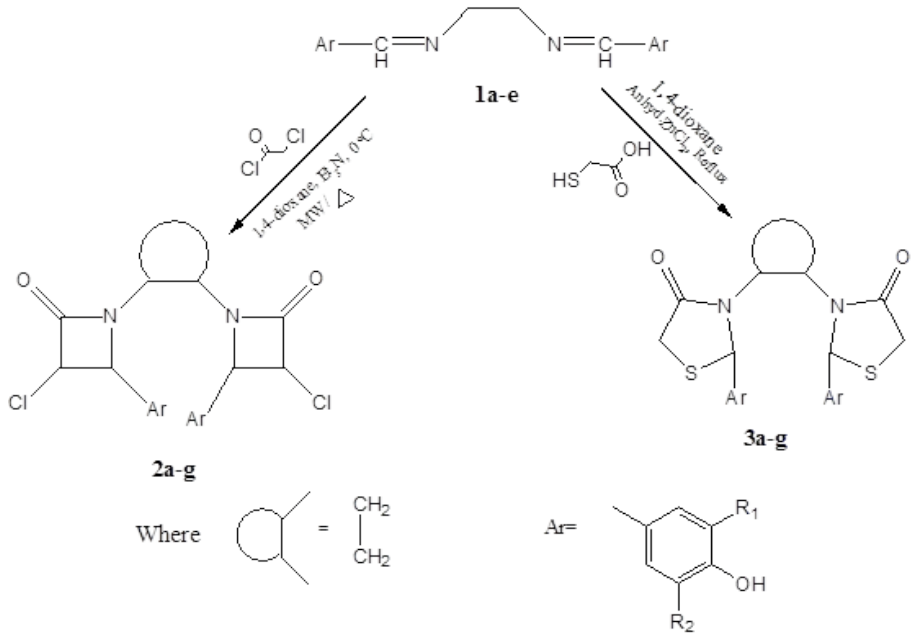

Scheme 1: Synthesis of some novel derivatives of bis-2-azetidinones and bis-4-thiazolidinones

The DPPH is a stable radical that can accept hydrogen radical to become a stable diamagnetic molecule. Due to its odd electron, alcoholic solution of DPPH shows a strong absorption at 517 nm. Therefore, DPPH readily reacts with reducing agent to yield colorless 2, 2'-diphenyl -1-picrylhydrazine. Reduction of the DPPH radicals can be determined quantitatively by measuring the decrease in absorbance at 517 nm.

Nitric oxide is generated by sodium nitroprusside in solution. In the presence of an antioxidant, the amount of NO generated will be less. The excess of NO estimated by Griess reagent, which is composed of the mixture of H_2SO_4 and naphthylethylene diamine.

The results of antioxidant activity expressed as IC50 value with two different antioxidant agents are shown in Table 3. The compounds 2c, 2f, 3c and 3f were tested using DPPH scavenging method and they showed IC50 value at 70.20, 70.28, 70.30, and 70.13 μM, when compared with that of the standard ascorbic acid at 69.08 μM, respectively. However the compound 2d and 2e did not show significant activity. Further, the antioxidant studies carried out using NO scavenging method, the only compounds 2c, 2g, 3c, and 3g showed IC50 value at 92.10, 91.25, 92.00 and 92.20 μM in comparison with standard, respectively. The compounds 2e and 3e did not show antioxidant activity.

Table 1: Physical and analytical data for bis-2-azetidinones.

Entry	R_1	R_2	mp, ^{0}C	% yield, CM	% yield, MW
2a	OEt	H	158	68	80
2b	OEt	Br	210	70	85
2c	OEt	I	220	75	90
2d	OMe	H	150	80	95
2e	OMe	Br	175	68	85
2f	OMe	Cl	180	70	84
2g	OMe	I	200	72	85

NB: CM: Conventional method, MW: Microwave method.

Table 2: Physical and analytical data for bis-4–thiazolidinones.

Entry	R_1	R_2	mp, ^{0}C	% yield, CM	% yield, MW
3a	OEt	H	178	70	85
3b	OEt	Br	190	75	85
3c	OEt	I	160	75	90
3d	OMe	H	155	80	95
3e	OMe	Br	215	75	85
3f	OMe	Cl	185	70	84
3g	OMe	I	170	74	85

Table 3: Antioxidant activity of bis- 2-azetidinones and bis-4-thiazolidinones.

Entry	DPPH scavenging (μM)	NO scavenging (μM)
2a	78.07	97.89
2b	85.27	105.64
2c	70.20	92.10
2d	NSA	146.97
2e	170.12	165.24
2f	70.28	96.28
2g	126.41	91.25
3a	83.59	116.93
3b	73.09	94.68
3c	70.30	92.00
3d	78.53	99.14
3e	NSA	107.47
3f	70.13	96.10
3g	125.15	92.20
Standard	69.08*	91.05*

Conclusion

In conclusion, the salient feature of our approach is coupling microwave with keeping modernization over classical procedure for the synthesis of bis-2-azetidinones and bis-4-thiazolidinones. The microwave technique is found to be efficient and cheap for the synthesis of mentioned compounds. In continuation of previously published results [32] and as a part of our research work, focus has been given on the development of new bis-2-azetidinones and bis-4-tiazolidinones as a bioactive agents. Synthesis and preliminary antioxidant screening of new bis-2-azetidinones and bis-4-thiazolidinones have been demonstrated. The presence of halogen atom in the compounds provides a positive influence on antioxidant activity. Owing to encouraging results, it was found that the synthesized compounds have broader value of activity than standard used for screening of antioxidant activity. The electronic effect also played a role in activity, as can be screen for the compounds having electron donor character such as –OEt, -OMe and –OH. Thus in future, this class of compounds may be used as templates for generating better lead molecules as a antioxidant agents.

Acknowledgment

The authors gratefully acknowledge to Principal, N.E.S. Science College, Nanded, for providing laboratory facilities and Director Indian Institute of Chemical Technology (IICT), Hyderabad for providing necessary instrumental facilities.

References

[1] Dave T, Purohit D, Joshi S. Synthesis and pharmacological study of thiazolidinones and mannich bases of 4-amino-3-mercapto-5-pyridin-3'-yl-[1,2,4]triazole. Indian J. Chem. 2007; 46B: 352-6.

[2] Patel R, Chikhalia, K. Synthesis and biological activity of some 2,4,6-trisubstituted- 1,3,5-s-triazines. J. Indian Chem. Soc. 2003; 80: 138-40.

[3] Kumar V, Nagraja T, Shameer H, Jayachandran E, Sreenivasa G. N – Substituted–3 –chloro– V, Nagaraja 2-azetidinones: Synthesis and characterization of new novel anti-inflammatory agents. Journal of Pharmaceutical Sciences and Research. 2009;(1): 83-92.

[4] Udupi R, Kasinath N, Bhat A. Synthesis and biological activity of some 2-(6-methoxy Napthyl) propionamido azetidine-2-ones. Indian J. Heterocycl. Chem. 1998; (17): 221-4.

[5] Samadhiya P, Sharma R, Srivastava S, Srivastava S. Synthesis and biological evaluation of 4-thiazolidinone derivatives as antitubercular and antimicrobial agents. Arebian Journal of chemistry. 2014,(7):657-65.

[6] Chavan A, Pai N. Synthesis and Biological Activity of N-Substituted-3-chloro-2-azetidinones Molecules. 2007; (12): 2467-77.

[7] Havaldar F, Mishra S. Azetidin-2-ones and thiazolidin-4-ones as potential antimicrobial agents. Indian J. Heterocycl. Chem. 2004; (13): 197.

[8] Patel K, Metha A. Synthesis and antifungal activity of azetidinones and thiazolidinones derivative of of 2,3- amino-6- (2-naphthalenyl) thiazolo [3, 2-d] thiadiazole EJChem. 2006; (3): 267-73.

[9] Trautman H, Longe L. The Synthesis Disubstituted-4-thiazolidones J. Am. Chem. Soc. 1948; (70): 3436-9.

[10] Surray A. 4-Thiazolidones. IV. The Preparation of Some 3-Alkylaminoalkyl-2-aryl Derivatives J. Am. Chem. Soc. 1949; (71): 3354-6.

[11] Patel N, Shaikh F. Synthesis and antimicrobial activity of new 4-thiazolidinone derivatives containing 2-amino-6-methoxybenzothiazole. Saudi. Pharm. J.2010;(18):129-36.

[12] Doran W, Sholen H. Dialkyl thiazolidinones J. Org. Chem. 1938;(3): 193-7.

[13] Sayed B. Synthesis and biological activity of some new 5-hydrothiazolo[4,3-b]- (thia) 1,3,4-oxa diazoles and 5-hydrothiazolo[3,4-b]-1,2,4-triazoles containing 1,2,3-selena(thia)diazole moiety. Acta Pol Pharma. 1991;(13): 48.

[14] Yadav R, Srivastav S, Srivastav S. synthesis, antimicrobial and anti-inflammatory activitiy of 4-oxothiazolidines and their 5-arylidines. Indian J. Chem. 2005; (44B): 1262-6.

[15] Oza H, Joshi D, Parekh H. Synthesis and antitubercular activitiy of novel thiazolidinone derivatives. Indian J. Chem. 1998; (37B): 822-5.

[16] Rawal R, Tripathi R, Katti S, Pennacouque C, Clercq E. Design,synthesis, and evaluation of 2-aryl-3-heteroaryl-1,3-thiazolidin-4-ones as anti-HIV agents.BiooorgMedchem.2007;(15): 1725-31.

[17] Patel R, Desai P, Desai K, Chikhalia K. Synthesis of pyrimidine based thiazolidinones and azetidinones: Antimicrobial and antitubercular agens. Indian J. Chem. 2006; (45B): 773-8..

[18] Solankee A, Patel K, Patel R. A facile synthesis and studies of some new 4-thiazolidinones and 5-arylidines. Pelagia Research Library; 2012, (3): 117-22.

[19] Zangade S, Mokle S, Shinde A, Vibhute Y. An atom efficient, green synthesis of 2-pyrazoline derivatives under solvent-free conditions using grinding technique. Green Chem. Lett. Rev. 2013; (6): 123-7.

[20] Zangade S, Shinde A, Patil A, Vibhute Y. An efficient and facile ring closure of 2′-hydroxychalcones under irradiation of tungsten light. EurJChem. 2012; (3): 208-10.

[21] Karamunge K, Sayed M., Vibhute A, Vibhute Y. Synthesis of some new chalcones, pyrazolines and acetyl pyrazolines derived from piperonal and halogenohydroxy acetophenones as antimicrobial agents. J. Indian. Chem. Soc. 2011; (88): 443.

[22] Zangade S, Mokle S, Chavan S, Vibhute Y.. 2-Methoxyethanol as an alternative reaction solvent for the synthesis of 1,5-benzodiazepines under microwave irradiation. Orbital: Electronic J. Chem. 2011; (3): 144-9.

[23] Zangade S, Shinde A, Vibhute A, Vibhute Y. An Improved Synthesis And Biological Evaluation Of Some New 4,5-dihydro-pyrazole-1-Carbaldehyde Derivatives Pak. J. Chem. 2012; (2): 1-6.

[24] Bhusare S, ShindeA, Pawar R, Vibhute Y. Synthesis and antimicrobial activity of Schiff bases, 4-thiazolidinones and 2-azetidinones. Indian J. Pharm. Sci. 2004; (66): 228-31.

[25] Pawar R, Andurkar N, Vibhute Y. Studies on synthesis and antibacterial Schiff bases, 4-thiazolidinones and 2-azetidinones. J.Indian Chem. Soc. 1999; (76): 271-2.

[26] Shinde AT, Zangade SB,Chavan SB, Vibhute AY, Nalwar YS, Vibhute YB. A Practical Iodination of Aromatic Compounds by Using Iodine and Iodic Acid. Synth. Commun. 2010; (40): 3506-13.

[27] Varma S. A solvent-free organic synthesis. Using supported reagents and microwave irradiation. Green Chem. 1999; (1): 43-5.

[28] Borah R, Kalita D, Sarma J. Microwave promoted selective preparations of acetals and esters from aldehydes. Indian J. Chem. 2002; (41B); 1032-36.

[29] Narl R, Rao M. Scavenging of free- radicals and inhibition of lipid peroxidation by 3-phenylsyndone. J.pharm. pharmacol. 1995; (47): 623-28.

[30] Kaur I, Geetha T. Screeninig methods for antioxidants-a review. Mini Reviews in Med.Chem. 2006; (6): 305-9.

[31] Chavan S, Zangade S, Mokle S, Vibhute Y. Synthesis of new bis-schiff bases via environmentally benign grindstone technique. Der Pharma Chemica, 2010; (2): 139-43.

[32] Shinde A, Zangade S, Chavan S, Vibhute Y. Microwave induced synthesis of bis-schiff bases from propane-1,3-diamine as promising antimicrobial analogs. Org.Commun, 2014; (7): 60-7.

Research Article
http://dergipark.ulakbim.gov.tr/jotcsa
JOTCSA, volume 2, issue 4 (2015), pp. 32-41

Synthesis and characterization of near-IR absorbing metal-free and zinc(II) phthalocyanines modified with aromatic azo groups

Mukaddes Özçeşmeci[a]
[a]Department of Chemistry, Istanbul Technical University, Maslak, 34469 Istanbul, Turkey
Corresponding author. E-mail: selcukoglu@itu.edu.tr. Tel: +90 212 285 7308; Fax: +90 212 285 6386

Abstract: Metal-free and zinc(II) phthalocyanine complexes bearing peripheral (E)-4-((2-hydroxynaphthalen-1-yl)diazenyl) units have been synthesized. Novel phthalonitrile derivative required for the preparation of phthalocyanine complexes was prepared by coupling 4-aminophthalonitrile and 2-naphthol. The structures of these new compounds were characterized by using elemental analyses, proton and carbon nuclear magnetic resonance, fourier transform infrared spectroscopy, ultraviolet–visible spectrophotometry, fluorescence spectrophotometry, and mass spectrometry. In the UV-Vis spectra a broad absorption band appears for phthalocyanine complexes at around 450–500 nm resulting from the azo-group introduced onto the phthalocyanine ring. The photophysical properties of metal-free and zinc(II) phthalocyanines were studied in tetrahydrofuran.

Submitted: April 9, 2015. **Revised:** May 1, 2015. **Accepted:** May 5, 2015.

Keywords: Phthalocyanines; synthesis; 2-naphthol; azobenzene; fluorescence.

Introduction

Organic colorants are being extensively studied because of numerous advantageous properties with many areas of possible applications. Phthalocyanines (Pcs) are important classes of these organics which have a highly conjugated pi-electron system. Interest of the Pcs still arises due to their excellent chemical and physical properties which give potential application in many fields of science and technology such as non-linear optics, gas sensors, electrocatalysis, solar cells, and sensitizers for photodynamic cancer therapy [1-6]. Pcs have high photosensitivity in the near-infrared region (650–850 nm). However, they exhibit a low optical absorption in the visible region (450–650 nm), and cannot be used in white light imaging processes. These properties of Pcs may be modulated by introducing substituent groups on peripheral, non-peripheral or axial positions, changing the symmetry of the Pc molecule, or introducing different metal cations into the cavity of the Pc ring [7-10].

Another class of organic colorants is azo compounds, are used in various areas, such as textiles, electro-optical devices, lasers, and ink-jet printers. They consist of one or more conjugated chromophore azo (–N=N–) groups in their structures. Due to their conjugated structures, azo compounds show intense absorptions in the visible region (450–650 nm) [11-13].

Although many kinds of Pcs and azo compounds have been widely used in many fields, azo group substituted Pcs are still scarce [14-17]. When Pcs and azo groups are included in the same framework, the components bring along their useful properties to the whole molecule. We therefore initiated a study on the mixed arrays of Pcs and azo compounds. In this study, we have reported synthesis and characterization of azo group modified Pcs containing naphthyl groups on the periphery.

Materials and Methods

All chemicals and reagents were purchased from major suppliers and used without any further purification. All reported ^{1}H NMR and ^{13}C NMR spectra were recorded on an Agilent VNMRS 500 MHz spectrometer. Chemical shifts (δ, ppm) were determined with TMS as the internal reference. FT-IR spectra were recorded on a Perkin-Elmer Spectrum One FT-IR (ATR sampling accessory) spectrometer, electronic spectra were recorded on a Scinco LabProPlus UV-Vis spectrophotometer. Fluorescence spectra were recorded on a Perkin-Elmer LS55 fluorescence spectrophotometer. Mass spectra were measured on a Bruker microflex LT MALDI–TOF MS spectrometer and Perkin Elmer Clarus 500 mass spectrometer in positive electron impact mode. The isotopic patterns for all assigned signals are in agreement with the calculated natural abundance. Data have been given for the most abundant isotope only. Melting points were determined on a Büchi Melting Point B-540 apparatus. Elemental analyses were performed on a Thermo Flash EA 1112. The homogeneity of the products was tested in each step by TLC (SiO_2). 4-Aminophthalonitrile was prepared according to the reported procedure [16].

Synthesis

Synthesis of (E)-4-((2-hydroxynaphthalen-1-yl)diazenyl)phthalonitrile (1)

4-Aminophthalonitrile (0.715 g, 5.0 mmol) was stirred and dissolved in a mixture of 10 mL of deionized water and 16 mL of concentrated hydrochloric acid until a clear solution was obtained. This solution was cooled to 0–5 °C, and then a solution of $NaNO_2$ (0.552 g, 8.0 mmol) in 10 mL of deionized water was added dropwise to the first solution. On the other hand, 2-naphthol (0.720 g, 5.0 mmol) was dissolved in 5 mL of 10% NaOH, cooled to 0–5 °C and then added to the solution of 3,4-dicyanobenzenediazonium chloride in small portions. Solid product immediately precipitated. The resulting mixture was stirred for further an hour at room temperature. The precipitate was filtered off, washed several times with water. The product was purified by crystallization with from ethanol. Yield: 0.641 g (43%); mp > 200 °C; anal. calcd. for $C_{18}H_{10}N_4O$: C, 72.48; H, 3.38; N, 18.78%. Found: 72.59; H, 3.39; N, 18.76%. IR: ν_{max}, cm^{-1} 3182 (OH), 3056 (Ar-CH), 2226 (C≡N), 1597 (C=C), 1479 (N=N). ^{1}H NMR (DMSO-d_6): δ, ppm 10.28 (s, H, -OH) 8.58 (d, H, Ar-H), 8.28 (s, H, Ar-H), 8.02 (m, 4H, Ar-H), 7.59 (t, H, Ar-H), 7.11 (d, H, Ar-H), 7.05 (d, H, Ar-H). ^{13}C NMR (DMSO-d_6): δ, ppm 158.53 (aromatic C), 153.49 (aromatic C-OH), 146.53 (aromatic C-H), 135.11 (aromatic C-H), 130.37 (aromatic C-H), 129.48 (aromatic C), 129.01 (aromatic C-H), 128.38 (aromatic CH), 128.33 (aromatic C-H), 127.87 (aromatic C), 126.51 (aromatic C-H), 126.11 (aromatic C), 123.50 (aromatic C), 123.16 (aromatic C-H), 120.22 (aromatic C), 116.35 (aromatic C), 115.72 (C≡N), 114.87 (C≡N). UV-Vis (THF): λ_{max}, nm (log ε) 310 (4.43), 447 (4.62). MS (EI^+): m/z 298.0 $[M]^+$.

Metal-free phthalocyanine (2)

Metallic lithium (0.134 g, 19.291 mmol) was suspended in 2 mL of n-pentanol and heated at 90 °C with stirring until a homogeneous mixture containing lithium pentanolate was formed. Then phthalonitrile derivative 1 (0.200 g, 0.671 mmol) was added to the reaction mixture and temperature was raised to 140 °C. The mixture was stirred for additional two hours. After cooling to room temperature the green crude product was precipitated with water and then 2 mL of concentrated hydrochloric acid was added to this mixture. In this mixture, the Li_2Pc was converted into H_2Pc. The precipitate was filtered off and washed with methanol, ethanol, hexane, chloroform, and acetone then dried *in vacuo*.

Yield: 0.022 g (11%); mp > 200 °C; anal. calcd. for $C_{72}H_{42}N_{16}O_4$: C, 72.35; H, 3.54; N, 18.75%. Found: 72.45; H, 3.55; N, 18.71%. FT-IR: ν_{max}, cm-1 3257 (NH), 3182 (OH), 3056 (Ar-CH), 1597 (C=C), 1479 (N=N). 1H NMR (DMSO-d6): δ, ppm 11.24 (s, 4H, OH), 8.37–6.65 (br, 36H, Ar-H), -4.03 (bs, 2H,-NH). UV-Vis (THF): λ_{max}, nm (log ε) 330 (4.50), 525 (4.63), 658 (4.51), 727 (4.54). MS (MALDI-TOF): m/z 1233.5 $[M+K]^+$.

Zinc(II) phthalocyanine (3)

A mixture of compound 1 (0.200 g, 0.671 mmol), $Zn(CH_3COO)_2$ (0.035 g, 0.190 mmol) and two drops of 1.8-diazabicyclo[5.4.0]undec-7-ene (DBU) in 2 mL of n-pentanol were heated and stirred at 140 °C in a glass sealed tube for 24 h under nitrogen atmosphere. The mixture was cooled down to room temperature and the solid product was precipitated by adding water. The precipitate was filtered off and washed with methanol, ethanol, hexane, chloroform, and acetone then dried *in vacuo*. Yield: 0.027 g (13%); mp > 200 °C; anal. calcd. for $C_{72}H_{40}N_{16}O_4Zn$: C, 68.71; H, 3.20; N, 17.81%. Found: C, 81.33; H, 3.90; N, 5.42%. IR: ν_{max}, cm^{-1} 3183 (OH), 3056 (Ar-CH), 1598 (C=C), 1479 (N=N). ^1H NMR (DMSO-d_6): δ, ppm 11.38 (s, 4H, OH), 8.52–6.66 (br, 36H, Ar-H). UV-Vis (THF): λ_{max}, nm (log ε) 345 (4.87), 440 (4.87), 734 (5.07). MS (MALDI-TOF): m/z 1260.7 $[M+2]^+$.

Results and Discussion

Synthesis and Characterization

In this study, the synthesis of (E)-4-((2-hydroxynaphthalen-1-yl)diazenyl)phthalonitrile (**1**) obtained by diazotization of 4-aminophthalonitrile and coupling with 2-naphthol in 10% NaOH solution. Diazonium cation was produced by treating the 4-aminophthalonitrile with nitrous acid ($NaNO_2$/HCl) at 0–5 °C for two hours. All spectroscopic data of newly synthesized phthalonitrile derivative (**1**) show a good agreement with proposed structures.

Cyclotetramerization of the phthalonitrile derivative (**1**) to the metal-free phthalocyanine (**2**) was accomplished by "Li method" in pentanol at reflux temperature in a sealed tube. The direct conversion of Li_2Pc to the metal-free complex **2** was achieved by addition of concentrated HCl to the solution of Li_2Pc. Compound **1** reacted with anhydrous $Zn(CH_3COO)_2$ in the presence of a catalytic amount of DBU via a template-oriented reaction in pentanol at refluxed temperature to obtain the zinc(II) phthalocyanine derivative (**3**) (Scheme 1). In this study, synthesized tetra-substituted phthalocyanine compounds (**2** and **3**) were obtained as mixture of four region-isomers of D_{2h}, C_s, C_{2v} and C_{4v} symmetries for similar physical and chemical properties. Both of synthesized phthalocyanines were soluble in DMF and DMSO, but insoluble in common organic solvents such as methanol, ethanol, hexane, chloroform, and acetone. The purification of complexes **2** and **3** was carried out by washing with methanol, ethanol, hexane, chloroform, and acetone. FT-IR, ^1H NMR, UV-Vis, elemental analysis, and mass characterization techniques were used to shed light into the structure of the novel Pcs (**2** and **3**). Spectral data of the novel compounds were in very good agreement with expected structures.

In the FT-IR spectrum of phthalonitrile derivative **1**, aromatic CH, aromatic C=C, azo group (N=N) stretching vibrations appeared at 3056, 1597, and 1479 cm^{-1}, respectively. The presence of the OH group was confirmed by the observation of broad OH stretching at 3182 cm^{-1}. In addition, the characteristic vibration of the C≡N appears at 2226 cm^{-1}, after conversion of the dinitrile into the phthalocyanine, the sharp peak for the C≡N vibration completely disappeared. The FT-IR spectra of the phthalocyanines **2** and **3** are very similar, except NH stretching band at 3257 cm^{-1} in the inner core of metal-free phthalocyanine **3**.

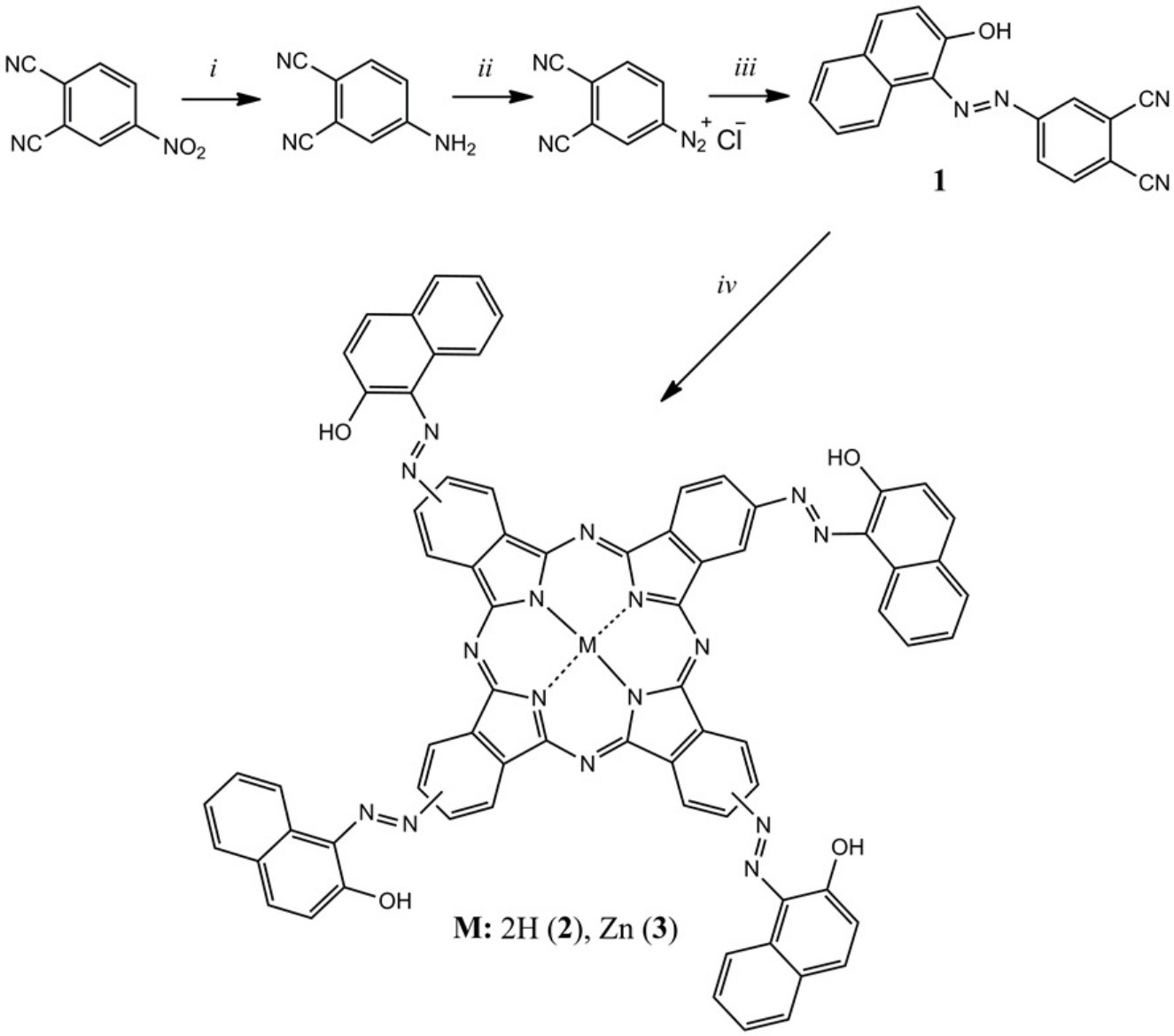

Scheme 1. Synthetic route for phthalonitrile (**1**) and phthalocyanines (**2** and **3**) (i: HCl, Fe, CH_3OH; ii: HCl, $NaNO_2$, 0 °C; iii: 2-naphthol, 10% NaOH, 0–5 °C; iv: a) Metallic lithium, n-pentanol, reflux; b) $Zn(CH_3COO)_2$, DBU, n-pentanol, reflux).

In the ^1H NMR analysis of **1** in DMSO-d_6, aromatic protons appear at 8.58, 8.28, 8.02, 7.59, 7.11, 7.05 ppm as a doublet, singlet, multiplet, triplet, doublet and doublet, respectively. The OH proton appeared at 10.28 ppm as singlet. The ^1H NMR spectra of the compounds **2** and **3** are somewhat broader than corresponding signals in the compound **1** due to aggregation of the phthalocyanine isomers which is frequently encountered at the concentrations used for NMR spectroscopy. The inner NH protons of **2** were also identified in the ^1H NMR spectra with a broad chemical shift at -4.03 ppm.

In ^{13}C NMR analysis of **1** in DMSO-d_6, aromatic carbons appear at 158.53, 146.53, 135.11, 130.37, 129.48, 129.01, 128.38, 128.33, 127.87, 126.51, 126.11, 123.50, 123.16, 120.22, and 116.35 ppm, C-OH group appeared at 153.49 ppm, nitrile carbons appeared at 115.72 and 114.87 ppm, respectively.

In the EI^+ mass spectrum of **1**, the presence of the characteristic molecular ion peak at m/z 298.0 $[M]^+$ confirmed the proposed structure. In the case of **2**, the molecular ion peak was found at m/z 1233.5 $[M+K]^+$ according to MALDI-TOF spectrum (Fig. 1). Also, the molecular ion peak for compound **3** found at m/z = 1260.7 $[M+2]^+$. The elemental analyses were satisfactory.

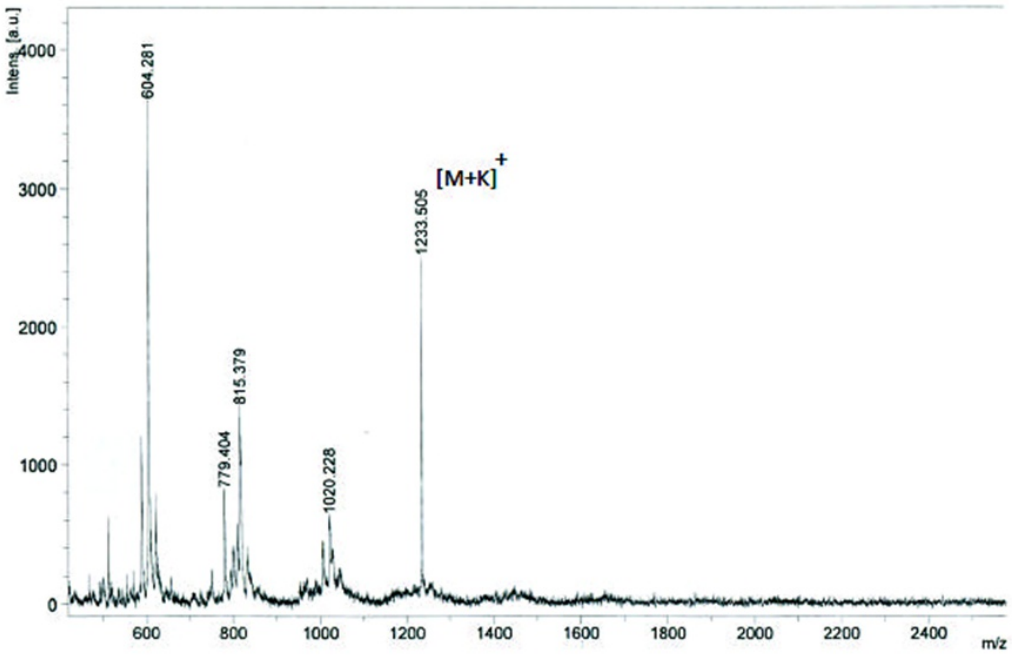

Figure 1. MALDI-TOF MS spectrum of compound **2**.

Ground state electronic absorption spectra

The simplest Pc unit is a 18-π electron system giving rise to electronic spectra with two strong absorption regions, one of them is in the UV region at about 300–400 nm (B band) and the other one is in the visible region at about 600–700 nm (Q band), both correlating to π-π* transitions. The absorption spectra of **2** and **3** in THF were shown in Figs. 3 and 4. The Soret bands are observed at 330 nm for complex **2** and 345 nm for complex **3**. The Q band, of complex **2**, is somewhat different from complex **3**, with a split Q band indicating lower symmetry (D_{2h}) of the metal-free derivative. The Q-band regions of the UV-Vis spectra are red-shifted into the near-IR region at 658 and 727 nm for complex **2** and at 734 nm for complex **3**. Due to the great extension of π-conjugation by four peripheral azo-dye moieties, the Q-bands of **2** and **3** are significantly red-shifted as compared to tetra-*tert*-butylphthalocyanines [4]. In addition, the extension of π-conjugation as well as aggregation in solution also leads to peak broadening. The precursor **1** and phthalocyanine complexes (**2** and **3**) produce intense absorptions from 450 to 550 nm (Figs. 2-4). This kind of additional absorptions is really uncommon, and might suggest some novel opto-electronic properties to the Pcs.

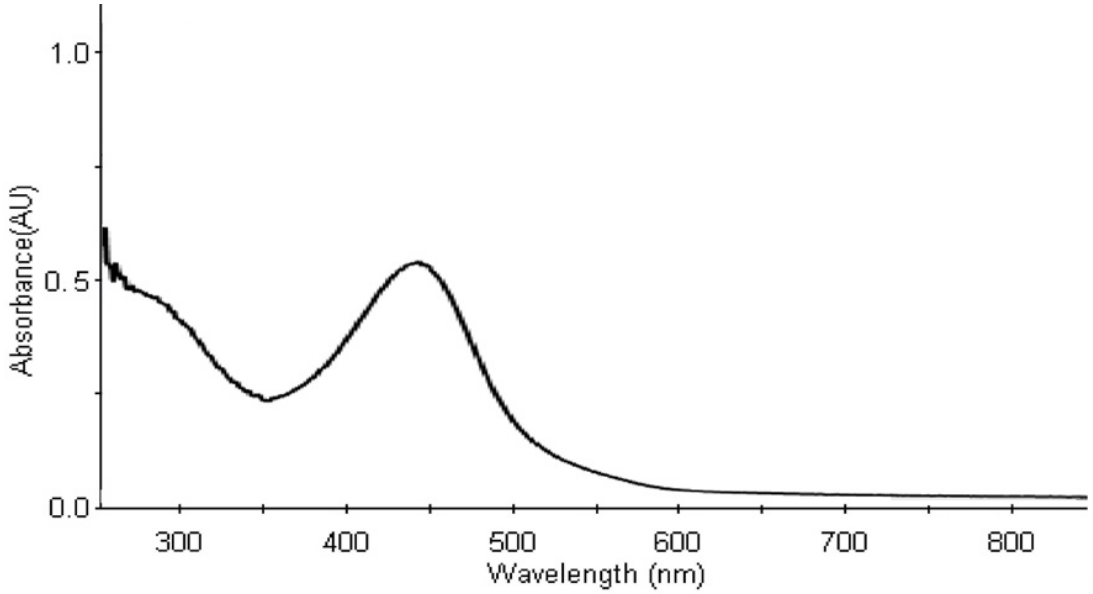

Figure 2. UV spectrum of **1** in THF.

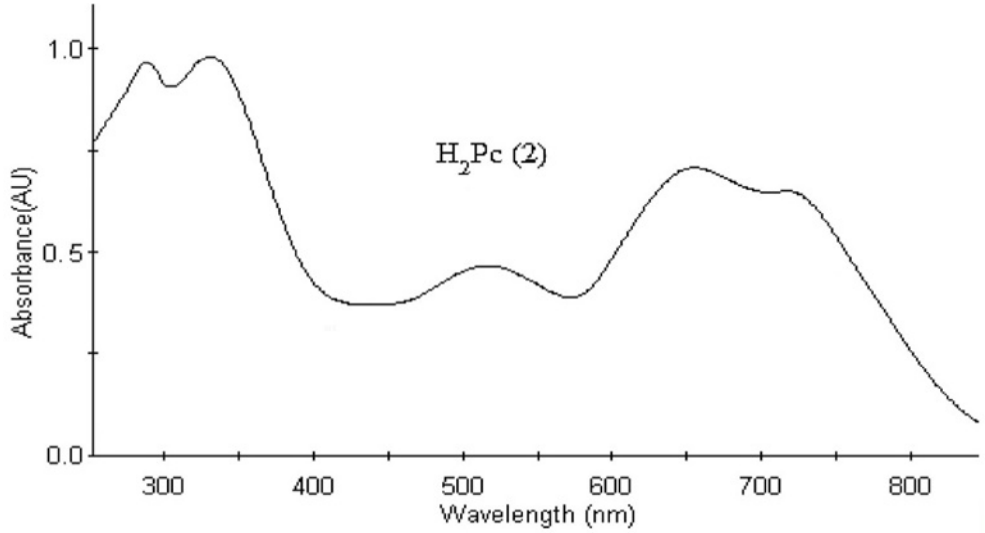

Figure 3. UV spectrum of **2** in THF.

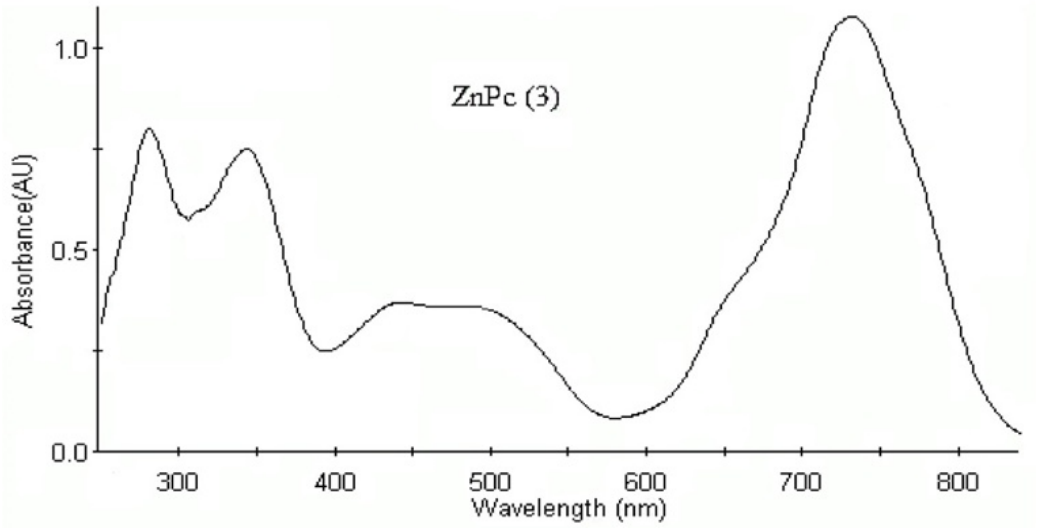

Figure 4. UV spectrum of **3** in THF.

Fluorescence spectra

The steady-state fluorescence spectra of phthalocyanine derivatives (**2** and **3**) were performed in THF, upon excitation at the 650 nm Q-band vibration for **2** and excitation at the 670 nm Q-band vibration for **3**. Emission around 744 nm for **2** and 755 nm for **3** (Fig. 5), occurred almost entirely from the phthalocyanine moiety. The Q bands of phthalocyanine derivatives' (**2** and **3**) luminescent spectra are red-shifted when compared to the corresponding peripherally substituted phthalocyanine complexes. The red-shifts observed in emission maxima are 40-60 nm bathochromically shifted in comparison with peripherally substituted phthalocyanine complexes [19]. Essentially, the energy gap (ΔE) between the S_0 and S_1 becomes smaller, resulting a bathochromic shift [19].

The excitation spectra of **2** and **3** were similar to absorption spectra and both were mirror images of the fluorescent spectra in THF. The proximity of the wavelength of the Q-band absorption to the Q-band maxima of the excitation spectra for ZnPcs suggest that the nuclear configurations of the ground and excited states are similar and are not affected by excitation in THF [20-22]. Excitation spectra of H_2Pc (**2**) show two shoulders in the red spectral region because of the lowering of symmetry [23].

Comparative method [Eq. (1)] was used to determine the quantum yields of the compounds (**2** and **3**) as described in [24, 25]. In this method, the quantum yield of a compound is determined by using a standard which has similar fluorescence properties as the tested compound has. All measurements of the standard and the compound must be performed at the same environmental conditions with the same instrumental settings.

$$\Phi_F = \Phi(Std)\frac{FA_{Std}\eta^2}{F_{Std}A\eta^2_{Std}} \quad (1)$$

Where F and F_{Std} are the areas under the fluorescence curves of phthalocyanines derivatives and the standard, respectively. A and A_{Std} are the respective absorbance of the sample and standard at the excitation and η and η_{Std} are the refractive indices of solvents used for the sample and standard, respectively. ZnPc was employed as a standard in DMF (Φ_F = 0.23) [26]. The fluorescence quantum yield (Φ_F) values for the complexes were found to 0.14 for H_2Pc (2) and 0.19 for ZnPc (3). The Φ_F values of all the studied Pc complexes are lower than unsubstituted ZnPc. It implies that the presence of the substituents (azo group) certainly results in fluorescence quenching, due to enhancement of intersystem crossing (ISC) by the presence of a heavier azo-naphthol groups in these complexes [27]. The Stokes' shifts ranged from 15 to 20 nm, typical of Pc complexes [28-29].

Conclusion

In this study, modified phthalocyanines having azo group and bearing naphthol units on the periphery were successfully prepared. The new compounds were characterized by using elemental analyses, ^{1}H NMR, UV-Vis and FT-IR spectroscopy and mass spectrometry. The results confirmed their proposed structures. The complexes (**2** and **3**) have good solubility in THF, DMF and DMSO. The Q bands of the phthalocyanine complexes (**2** and **3**) were red-shifted compared to the peripherally substituted metal-free and zinc phthalocyanine complexes. These complexes (**2** and **3**) produce an intense absorption from 450 to 500 nm and might suggest for some novel opto-electronic devices.

The fluorescence behaviors of the phthalocyanine complexes (**2** and **3**) were studied in THF. Generally, the Φ_F values of these complexes are lower than unsubstituted ZnPc.

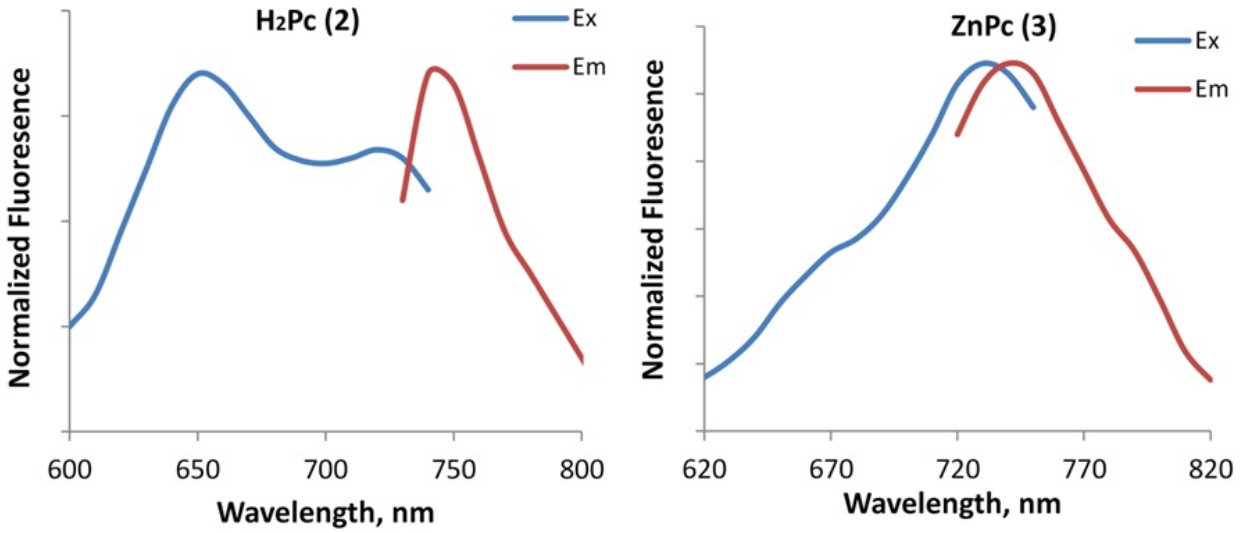

Figure 5. Excitation and emission spectra of **2** and **3** in THF. Excitation wavelengths: 650 nm for **2** and 670 nm for **3**.

Acknowledgments

This work was supported by the Research Fund of the Istanbul Technical University.

References

[1] De la Torre G, Vázquez P, Agulló-López F, Torres T. Phthalocyanines and related compounds:organic targets for nonlinear optical applications. Journal of Materials Chemistry. 1998;8(8):1671–83. DOI: 10.1039/A803533D.

[2] Harbeck M, Taşaltın C, Gürol I, Musluoğlu E, Ahsen V, Öztürk ZZ. Preferential sorption of polar compounds by fluoroalkyloxy substituted phthalocyanines for the use in sorption based gas sensors. Sensors and Actuators B: Chemical. 2010 Oct;150(2):616–24. DOI: 10.1016/j.snb.2010.08.031.

[3] Koca A, Özçeşmeci M, Hamuryudan E. Substituents Effects to the Electrochemical, and In Situ Spectroelectrochemical Behavior of Metallophthalocyanines: Electrocatalytic Application for Hydrogen Evolution Reaction. Electroanalysis. 2010 Apr 22;22(14):1623–33. DOI: 10.1002/elan.200900545.

[4] Leznoff CC, Lever ABP. Phthalocyanines: Properties and Applications, vols.1–4, VCH, Weinheim, 1998.

[5] Ragoussi M-E, Yum J-H, Chandiran AK, Ince M, de la Torre G, Grätzel M, et al. Sterically Hindered Phthalocyanines for Dye-Sensitized Solar Cells: Influence of the Distance between the Aromatic Core and the Anchoring Group. ChemPhysChem. 2014 Apr 14;15(6):1033–6. DOI: 10.1002/cphc.201301118.

[6] Horne TK, Abrahamse H, Cronjé MJ. Investigating the efficiency of novel metallo-phthalocyanine PDT-induced cell death in MCF-7 breast cancer cells. Photodiagnosis and Photodynamic Therapy. 2012 Sep;9(3):215–24. DOI:10.1016/j.pdpdt.2011.12.008

[7] Burnham PM, Cook MJ, Gerrard LA, Heeney MJ, Hughes DL. Structural characterisation of a red phthalocyanine. Chemical Communications. 2003;(16):2064. DOI: 10.1039/B304173P.

[8] Àlvarez Micó X, Vagin SI, Subramanian LR, Ziegler T, Hanack M. New Unsymmetrical Zinc-Phthalocyanine Conjugated with One Azo-Dye Moiety: Synthesis via Opening the Fused Triazole Ring and Spectral Properties. European Journal of Organic Chemistry. 2005 Oct;2005(20):4328–37. DOI: 10.1002/ejoc.200500237.

[9] Güzel E, Atsay A, Nalbantoglu S, Şaki N, Dogan AL, Gül A, et al. Synthesis, characterization and photodynamic activity of a new amphiphilic zinc phthalocyanine. Dyes and Pigments. 2013 Apr;97(1):238–43. DOI:10.1016/j.dyepig.2012.12.027.

[10] Uslan C, Şebnem Sesalan B. The synthesis, photochemical and biological properties of new silicon phthalocyanines. Inorganica Chimica Acta. 2013 Jan;394:353–62. DOI:10.1016/j.ica.2012.08.004.

[11] Hunger K. Industrial Dyes: Chemistry, Properties, Wiley-VCH, Germany, Weinheim, 2003.

[12] Hsueh C, Chen B. Comparative study on reaction selectivity of azo dye decolorization by Pseudomonas luteola. Journal of Hazardous Materials. 2007 Mar 22;141(3):842–9. DOI:10.1016/j.jhazmat.2006.07.056.

[13] Egli R. Colour chemistry. In The design and Sythesis of Organic Dyes and Pigments, Peters AT, Freeman, HS. (Eds.), Elsevier, London (1991) 193–223.

[14] Yenilmez HY, Okur Aİ, Gül A. Peripherally tetra-palladated phthalocyanines. Journal of Organometallic Chemistry. 2007 Feb;692(5):940–5. DOI: 10.1016/j.jorganchem.2006.10.044.

[15] Yazıcı A, Ateş D, Bekaroğlu Ö, Kobayashi N. Synthesis and characterization of novel azo-bridged Zn(II) and Co(II) bisphthalocyanines. Journal of Porphyrins and Phthalocyanines. 2006 Sep;10(09):1140–4. DOI: 10.1142/S1088424606000491.

[16] Liu Y, Lin H, Li X, Li J, Nan H. Photoinduced electron transfer in panchromatic zinc phthalocyanine–azobenzene dyad. Inorganic Chemistry Communications. 2010 Jan;13(1):187–90. DOI:10.1016/j.inoche.2009.11.012.

[17] Özçeşmeci İ, Tekin A, Gül A. Synthesis and aggregation behavior of zinc phthalocyanines substituted with bulky naphthoxy and phenylazonaphthoxy groups: An experimental and theoretical study. Synthetic Metals. 2014 Mar;189:100–10. DOI:10.1016/j.synthmet.2014.01.003.

[18] Makhseed S, Al-Sawah M, Samuel J, Manaa H. Synthesis, characterization and nonlinear optical properties of nonaggregating hexadeca-substituted phthalocyanines. Tetrahedron Letters. 2009 Jan;50(2):165–8. DOI:10.1016/j.tetlet.2008.10.102.

[19] Valeur B. Molecular Fluorescence Principles and Applications, Wiley-VCH, Germany, Weinheim, 2002.

[20] Özçeşmeci M, Özçeşmeci İ, Hamuryudan E. Synthesis and characterization of new polyfluorinated dendrimeric phthalocyanines. Polyhedron. 2010 Sep;29(13):2710–5. DOI: 10.1016/j.poly.2010.06.023.

[21] Durmuş M, Bıyıklıoğlu Z, Kantekin H. Synthesis, photophysical and photochemical properties of crown ether substituted zinc phthalocyanines. Synthetic Metals. 2009 Aug;159(15-16):1563–71. DOI: 10.1016/j.poly.2010.06.023.

[22] Gümrükçü G, Karaoğlan GK, Erdoğmuş A, Gül A, Avcıata U. A novel phthalocyanine conjugated with four salicylideneimino complexes: Photophysics and fluorescence quenching studies. Dyes and Pigments. 2012 Nov;95(2):280–9. DOI:10.1016/j.dyepig.2012.05.005.

[23] Özçeşmeci İ, Güney O, Okur Aİ, Gül A. New phthalocyanines containing bulky electron rich substituents. Journal of Porphyrins and Phthalocyanines. 2009 Jun;13(06):753–9. DOI: 10.1142/S1088424609000838.

[24] Göl C, Durmuş M. Investigation of photophysical, photochemical and bovine serum albumin binding properties of novel water-soluble zwitterionic zinc phthalocyanine complexes. Synthetic Metals. 2012 May;162(7-8):605–13. DOI: 10.1016/j.synthmet.2012.02.017.

[25] Ogunsipe A, Durmuş M, Atilla D, Gürek AG, Ahsen V, Nyokong T. Synthesis, photophysical and photochemical studies on long chain zinc phthalocyanine derivatives. Synthetic Metals. 2008 Dec;158(21-24):839–47. DOI: 10.1016/j.synthmet.2008.06.007.

[26] Scalise I, Durantini EN. Synthesis, properties, and photodynamic inactivation of Escherichia coli using a cationic and a noncharged Zn(II) pyridyloxyphthalocyanine derivatives. Bioorganic & Medicinal Chemistry. 2005 Apr;13(8):3037–45. DOI: 10.1016/j.bmc.2005.01.063.

[27] Lakowicz JR. Principles of Fluorescence Spectroscopy, (3rd ed.) Springer, Berlin, 2006.

[28] Masilela N, Nyokong T. Synthesis and physicochemical behavior of new low symmetry Ge, Ti and Sn phthalocyanines: Effect of central metal. Synthetic Metals. 2012 Dec;162(21-22):1839–45. DOI: 10.1016/j.synthmet.2012.07.028.

[29] Özçeşmeci M. Synthesis, photophysical and photochemical properties of metal-free and zinc(II) phthalocyanines bearing α-naphtholbenzein units. Journal of Organometallic Chemistry. 2014 Sep;767:16–21. DOI: 10.1016/j.jorganchem.2014.05.015.

JOTCSA, volume 2, issue 4 (2015), pp. 42-52

Research Article

http://dergipark.ulakbim.gov.tr/jotcsa

Theoretical Investigations for the Behavior of Hydrotropes in Aqueous Solution

Rabah A. Khalil*, Al-hakam A. Zarari

Department of Chemistry, College of Science, University of Mosul, Mosul, Iraq.

E-mail: rakhalil64@yahoo.com

Abstract: The presented paper introduces an attempt for finding a theoretical model capable for describing the critical aggregation concentration (cac) for some hydrotropes (a series of sodium-p-n-alkylbenzoates, n=0-8). Such a proposal was carried out through theoretical calculations based on density functional theory (DFT) for estimating some physical properties which might be helpful for supporting the recent published report as all of these hydrotropes are considered as surfactant like (see doi: 10.1021/la2025846). The estimated physical properties can be divided to three classes according to their effect: steric properties such as volume and surface area, electronic properties such as polarizability, and hydrophobic properties such as log P which represents the ratio of concentrations of a compound in two phases of octanol and water. The results show that both steric and hydrophobic properties play major roles in predicting the cac for the presented hydrotropes. The best model was found between cac and tail polarizability (PT) according to the following relation: cac = 1.52-1.09log PT ; with r^2 equal to 0.96, S.E equal to 0.026 M and significant cross validation correlation coefficient (0.943). A unique feature of the presented model is containing only one descriptor with excellent statistical parameters. This actually supports the recent (above mentioned) published results of that all of these hydrotropes can be considered as surfactant-like. The suggested models were applied to some randomly selected surfactants with reasonable results. The results are generally suggesting for the possibility of estimating the cac or critical micelle concentration (cmc) for amphiphilic molecules using computational chemistry software.

Submitted: March 22, 2015. **Revised:** July 21, 2015. **Accepted:** July 23, 2015.

Keywords: Density functional theory (DFT), Qualitative structure property relationship (QSPR), Hydrotropes, Critical aggregation concentration (cac), Critical micelle concentration (cmc), Surfactant, Sodium-p-n-alkylbenzoates.

Introduction

In recent years, hydrotropes as amphiphilic organic molecules has long been a special topic due to their special characteristics, giving the possibility for their employment in many aspects [1, 2]. However, a clear and general definition of hydrotropes still need verification [3,4]. For instance, hydrotropes are divided into two classes from self-assembly point of view; surfactant-like and unlike. In other words, the chain length of hydrophobic part of hydrotrope plays the major role on the last classification. Recently, Hopkins Hatzopoulos et al.[5] investigated the physicochemical properties of a homologous series of sodium p-n-alkylbenzoates (Scheme 1). They stated according to their results of small angle neutron scattering (SANS) technique and surface tension analysis that all of these hydrotropes display as surfactant like behaviors with no regard to the chain length. Subsequently, they have supported this event through studying the effects of structure variation on physicochemical behavior of hydrotropes composed of sodium phenyl-n-alkanoates and cyclohexyl-n-alkanoates [6].

Actually, such a surprising phenomenon was attracted us for theoretical verification using quantum mechanical calculations. According to the literature, there is no theoretical study based on quantum mechanical methods that have been performed for hydrotropes. Such kind of a study was only found for surfactant molecules. For instance, Huibers studied the electrical charge distribution in some ionic surfactants using quantum chemical calculations [7]. He indicated that the partial charge distribution influences surfactant self-assembly and physical properties. Other publications based on employing the quantitative structure-property relationship (QSPR) have been found for a considerable number of anionic surfactants [7-14]. A part of complexity for the prediction of descriptors has been mostly shown by these investigations. For examples, the Kier and Hall descriptor was calculated indirectly through many parameters [13].

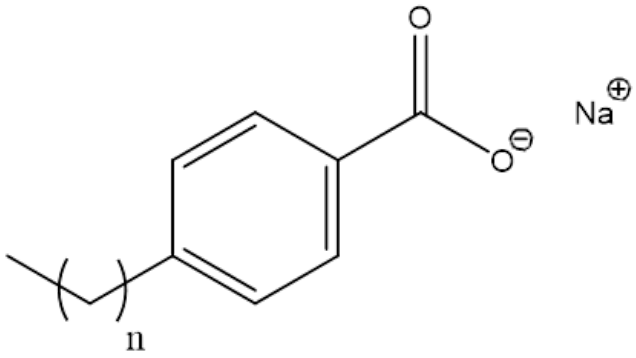

Scheme 1. Chemical structure of sodium p-n-alkylbenzoates; n=0-8.

Thus, the presented paper introduces theoretical investigations using density functional theory (DFT) and qualitative structure property relationship (QSPR) calculations that might be helpful for understanding the recent published results of hydrotropes [5]. It should be noted that we have recently used these hydrotropes to develop a theoretical model that used for evaluating the critical packing parameter of self-assembled amphiphilic molecules [15]. The obtained results were indirectly supporting that the members of all studied hydrotropes family may be considered as surfactant-like.

Theoretical section

The experimental cac values of used hydrotropes (sodium p-n-alkylbenzoates, n=0-8) were taken from Reference 5. The experimental cmc of all selected surfactants were taken from Reference 16.The chemical structural inputs for of all presented molecules and their models were prepared by using HyperChem 8.0.8 program package. Each of the structures was employed as a starting point for energy minimization using molecular mechanics MM2, semi-empirical PM3 and DFT methods according to our developed procedure that has already listed in the related published research [15]. In this method, a series of computational operations have been suggested in order to reach the best method from accuracy and time-consuming points of views. In other words, our treatments deal with relatively huge molecules (surfactants) which need long periods of time if one uses large or medium basis set for computation process. Therefore, considerable efforts have been paid in order to find an accurate method using small basis set. It has been found that the use of molecular mechanics for a conformational analysis and then a geometric optimization with DFT at relatively small basis set (3-21G) and B3LYP hybrid functional is a significant tool to search for the global minima [15].

This procedure eliminates the significance of using large and medium basis sets which therefore the time consumed for this process is comparatively very short. The selected properties of the presented molecules were estimated from their optimized structures Finally, Minitab program (MINITAB Release 14.1, www.minitab.com) was used for regression analysis of the calculated data.

Results and discussion

The recent observation by Hopkins Hatzopoulos et al. [5] with respect to SANS analysis showed that all hydrotropes (sodium p-n-alkylbenzoates, n=0-8) behaving as surfactant-like which has guided us to do theoretical investigations which might be helpful in illustrating such a phenomenon. In fact, the latter observation contradicts with the well-known assumption of that surfactant molecules must have chain of at least 8 carbon atoms in order to have self-assembled structure or following an "on-off" mode of aggregation. Table 1 lists the calculated theoretical parameters using DFT method for the presented compounds.

The results show no remarkable difference in head charge, tail charge, head surface area, charge on α-CH_2, polarizability of head, HOMO, LUMO for these hydrotropes. The reason for this may be attributed to the relatively low reactive side of the hydrocarbonic alkyl chain as saturated group in contrast to the head group which remains fixed for all of the presented hydrotropes. In other words, these parameters have no influence on the cac values of amphiphilic molecules. It is clearly shown (Table 1) the head volume increased in zigzag mode with increasing the tail length. Such non-linear mode which represents the charge of number of methylene groups from odd to even is not new here. This is due to the observation that the zigzag mode was already found for some physical properties of hydrocarbons particularly those of alkynes. However, the increase in head volume may be attributed to that the negative charge of the head is enhanced by increasing the number of CH_2 groups as considered as electron donor group. On the other hand, the results indicate that the Log P values which represent the ratio of concentrations of a compound in the two phases of a mixture of two immiscible solvents at equilibrium "octanol and water" increases with increasing tail length. For instance, compounds with high partition coefficients (high Log P) are preferentially distributed to hydrophobic compartment while hydrophilic compounds (low Log P) are preferentially found in the hydrophilic part. This can be attributed to the hydrophobic interactions through dispersion forces. On the other hand, the polarizability (α) was also increased with the increasing the number of CH_2 groups at the tail because α depends on the induced dipole moment which is increased with increasing number of CH_2 groups according to the following relation [17], where (μ_{ind}) is the induced dipole moment and (E) is the electric field strength.

$$\alpha = \mu_{ind} / E \ (C^2\ m^2\ J^{-1}) \quad (1)$$

Table 1. List of the calculated properties of the sodium p-n-alkylbenzoates (n=0-8) hydrotropes.

	Sodium p-n-alkylbenzoate (n=0-8) hydrotropes								
Property	**n = 0**	**n = 1**	**n = 2**	**n = 3**	**n = 4**	**n = 5**	**n = 6**	**n = 7**	**n = 8**
Head Charge (e)	-0.765	-0.768	-0.768	-0.767	-0.765	-0.767	-0.764	-0.767	-0.765
Tail Charge (e)	-0.338	-0.336	-0.340	-0.337	-0.339	-0.337	-0.339	-0.337	-0.337
Charge α-CH_2 (e)	non	-0.232	-0.224	-0.202	-0.206	-0.201	-0.206	-0.202	-0.206
Head Surface area $A^{\circ 2}$	93.29	93.53	92.77	93.01	93.45	93.89	93.60	94.06	93.89
Tail surface area$A^{\circ 2}$	181.48	213.28	240.49	269.73	303.02	331.38	366.79	395.39	427.66
Total surface area$A^{\circ 2}$	274.77	301.82	328.13	357.89	392.11	420.22	456.62	484.38	517.21
Head Volume $A^{\circ 3}$	947.8	1110.2	1098.5	1173.0	1135.3	1326.5	1404.5	1478.7	1322.5
Tail volume$A^{\circ 3}$	358.50	473.64	517.32	578.54	630.41	690.71	740.06	792.38	820.95
Total volume $A^{\circ 3}$	396.98	449.49	498.77	553.21	611.61	663.10	719.40	772.33	828.84
Chain length A°	3.50	5.02	6.10	10.46	8.62	10.00	11.20	12.56	13.76
Log P Tail	1.706	2.333	2.729	3.125	3.522	3.918	4.314	4.711	5.107
Log P Total	3.166	3.633	4.030	4.426	4.822	5.218	5.615	6.011	6.407
Polarizability of Head/ C^2 m^2 J^{-1}	3.842	3.842	3.842	3.842	3.842	3.842	3.842	3.842	3.842
Polarizability ofTail/ C^2 m^2 J^{-1}	8.695	11.882	13.717	15.552	17.387	19.222	21.057	22.892	24.727
Total polarizability C^2 m^2 J^{-1}	12.54	14.37	16.21	18.04	19.88	21.71	23.55	25.38	27.22
HOMO (eV)	-4.62	-4.62	-4.62	-4.63	-4.65	-4.64	-4.66	-4.64	-4.66
LUMO (eV)	3.93	3.84	3.84	3.83	3.77	3.81	3.75	3.80	3.74
[cac] [5]	0.480	0.320	0.300	0.280	0.200	0.090	0.048	0.024	0.011

In order to find the best relationship between the calculated values of physical properties with the practical values of cac (Table 1), a general correlation matrix which gathers all calculated properties has been formed. Indeed, such a matrix will be quite helpful in order to verify if there is any combination between the calculated parameters. For example, the property of refractivity is derived directly from the polarizability which was therefore neglected from Table 1. This can be considered as an important point while concerning with building a multi-parametrical model. Interestingly, the results of constructed matrix show according to statistical parameters there is only one descriptor which is quite enough for predicting the cac of the presented hydrotropes as exhibited in Table 2. Indeed, this gives an efficient support to the previous experimental results [5, 6] as all the investigated sodium salts hydrotropes possess 'on-off" mode of association with no regards to hydrophobic chain length. This event may be explained in terms of the phenomenon that the presence of sodium carboxylate group as a polar head which could acts as an anti-hydrophobic effect. In other words, the water molecules surrounding this polar group will decrease the hydrogen bonding between each other which then reduce the density of solution [18]. Then, the movement of hydrotropes within solution will be much easier in this state as the shorter hydrophobic chain length will be more efficient in contrast to that of longer. This is because of the fact that the neighboring water molecules will be relatively close to hydrophobic part of shorter chain, while, the hydrophobic interactions of the longer chain length play the major role for aggregation. Thus, all of these hydrotropes behave as surfactant-like.

Hence, four properties have been chosen as a single descriptor for each developed model possessing good statistics stability and predictive power. One of these properties represents the electronic effect (polarizability of tail) and two representing the steric effect (tail volume and tail surface area). While the last one (log P of tail) is considered as a measure of the amount hydrophobicity which increases with increasing tail length (number of CH_2 groups) as illustrated above. Moreover, this parameter can be considered as hydrophilic-lipophilic balance of a substance which reflects its partitioning behavior between a polar (water) and non-polar (oil) medium. In fact, there is a clear physical meaning realized from all of these equations as the cac decreases with increasing the number of $-CH_2$-group. It should be noted that all of above selected descriptors are representing the properties of the hydrophobic group (tail) which is in good agreement with theory of micellization.

The results show that the amounts of the intercepts are more than the cac of the shorter chain length which give an indication for the successfulness of all suggested models. On the other hand, the relationship between the experimental and calculated cac values for these four models (Table 2) signifies an apparent weak point that resulted from the negative values of cac for the longer alkyl chain length (lower cac value), as shown clearly in Figure 1. Indeed, such a problem can be also realized from the value of standard error for the above model which exceeds the value of cac for the lower cac molecule. Therefore, the investigations should be extended for another suitable model. Such a problem may suggest there is no perfect linearity between cac versus the selected physical properties. Therefore, the relationship should be improved through using some mathematical operators such as square root, log, exponential, and so on. The results of such curve fitting treatments indicate that the logarithmic operator is the proper one which gives the best statistical stability and predictive power for the three properties TVO, PT and LPT as illustrated in Table 3.

Furthermore, the latter curve-fitting process has solved the problem of the negative value for those best three models as shown clearly in Figures 2-4. The parameters of cross validation correlation coefficient (q^2) and standard deviation of residual between observed and calculated values of cac have been introduced (Table 3) due to the apparent closeness in the values of statistical parameters (r and S.E.) of these models. Indeed, the values of q^2 for these models are quite close to each other which they near to the top value (unity). However, the best model may be chosen with respect to the relatively best value of standard deviation between observed and fitted cac as given in Table 3. Hence, the model of polarizability of tail ([cac] = 1.52-1.09 log PT) is considered as the most powerful model for estimating the cac of the presented hydrotropes. In general, this model is quite significant from both of physical and statistical point of views.

Table 2. The best selected models obtained from the correlation matrix between cac and some of the calculated theoretical properties of hydrotropes with statistical parameters.

Property	Symbol	Model (y=a-bx)	r	S.E. (M)
Tail volume	TVO	[cac] = 0.840 -1.04×10^{-3}TVO	-0.988	0.032
Tail surface area	TSA	[cac] = 0.763 - 1.97×10^{-3}TSA	-0.972	0.040
Polarizability of tail	PT	[cac] = 0.714 -3.01×10^{-2}PT	-0.980	0.034
Log P of tail	LPT	[cac] = 0.687 - 0.141 LPT	-0.979	0.035

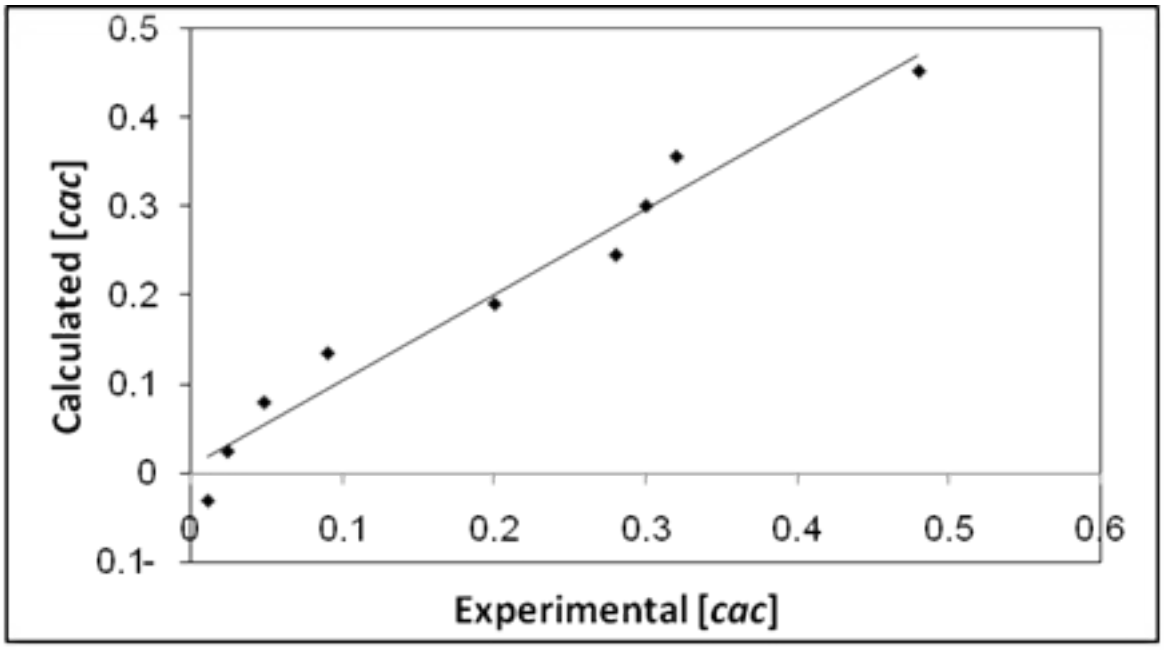

Figure 1. The relationship between experimental cac values and predicted cac of polarizability of tail (PT).

Table 3. The best selected models obtained from the treatment by curve-fitting for the relation between cac and some of the calculated theoretical properties of hydrotropes with statistical parameters.

Property	Symbol	Model	r	S.E. (M)	q^2	SD (M)
Tail volume	TVO	[cac] = 3.97-1.36 logTVO	-0.983	0.033	0.945	0.088
Polarizability of tail	PT	[cac] = 1.52-1.09 log PT	-0.981	0.033	0.943	0.026
Log P of tail	LPT	[cac] = 0.730-1.03 logLPT	-0.981	0.034	0.945	0.039

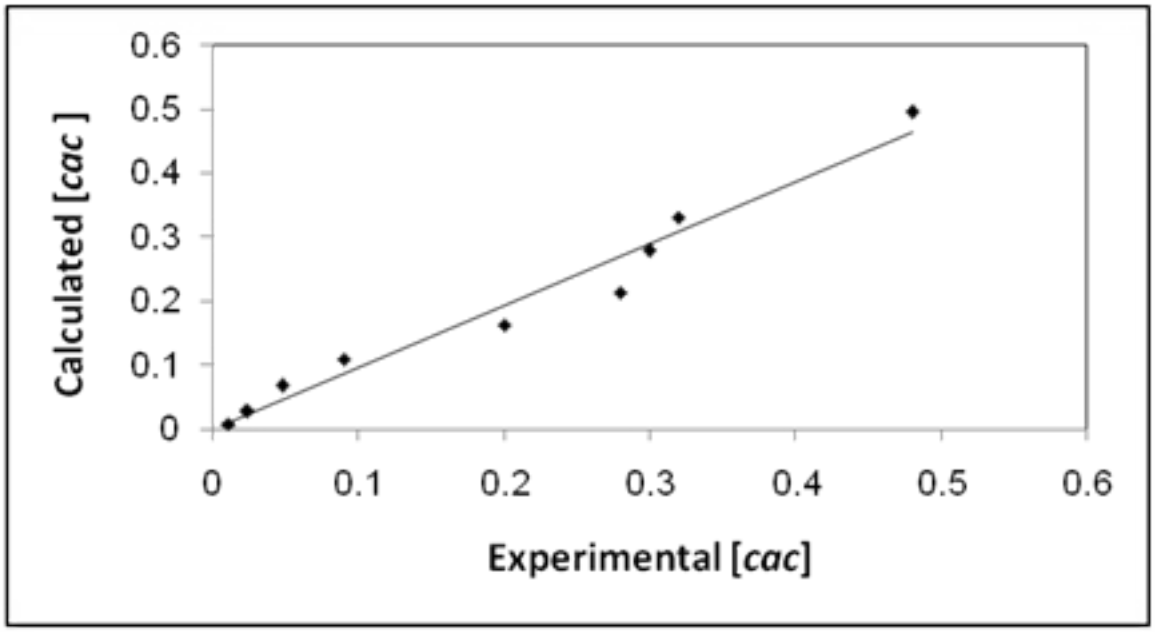

Figure 2. Relationship between experimental cac and calculated cac values from the logarithm of tail volume.

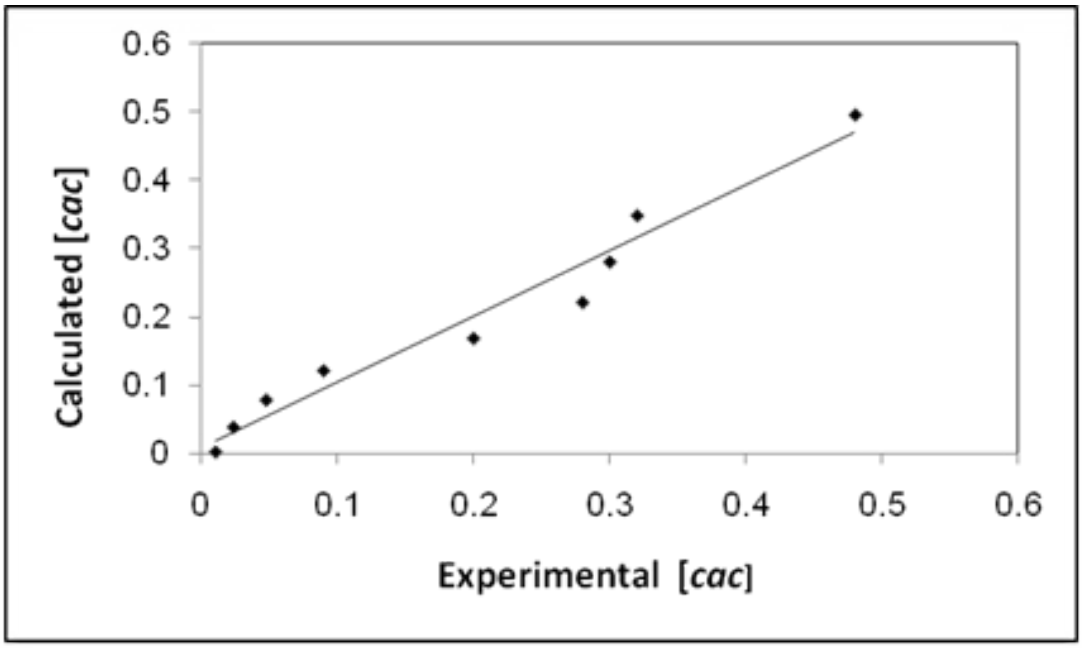

Figure 3. Relationship between experimental cac and calculated cac values from the logarithm of polarizability of tail.

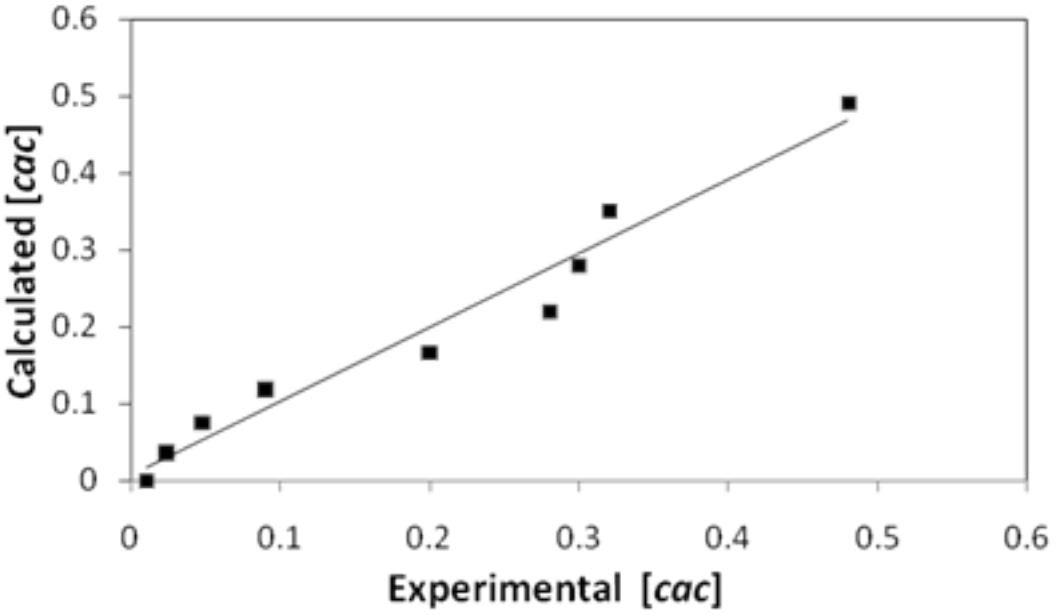

Figure 4. Relationship between experimental cac and calculated cac values from the logarithm of Log P of tail.

An application of the above selected three models for predicting critical micelle concentration (cmc) of two sets of different head groups of anionic surfactants was carried out as illustrated in Table 4. It is not surprising that the presented models are not applicable for estimating the cmc of ionic surfactants in contrast to cac of hydrotropes [19]. This can be attributed to the effect of presence of free gegen- or counter-ions which not exciting in hydrotropes systems. Furthermore, the presence of free gegen-ions could disturb the interactions between head groups which therefore deform the symmetry of micelle or aggregate system. Actually, the presence of these ions at Gouy-Ghapman layer [20] creates a real problem in computational investigations. This because the theoretical calculations estimate the properties of surfactant molecules in its monomer state as all these molecules are the same when they accumulated in micelle structure. It is apparent that the presented models are relatively more applicable for determining the cmc of sodium acetate micelle in contrast to that of sodium sulfate according to the values of statistical parameters as clearly shown in Table 4. This is because of the fact that the amount of free gegen-ions depends on the ionization of surfactant molecule. The relatively low ionization potential of sodium acetate surfactant decreases the probability of the presence of free gegen-ions in contrast to that of sodium sulfate. However, the values of standard deviation again suggest that the model of tail polarizability is relatively the best model for estimating the cmc of surfactants.

Table 4. Predicted *cmc* for some surfactants using the three models of Table 3 versus experimental *cmc*.

Surfactant	***cmc*[a] [M]**	**TVO (A^3)** **{*cmc*}[b]** **(Δ)[c]**	**PT(C^2 m^2 J^{-1})** **{*cmc*}[d]** **(Δ)[c]**	**LPT** **{*cmc*}[e]** **(Δ)[c]**
Sodium tatradecylsulfate	0.0021	1125.961 {-0.1800} (-0.1821)	27.912 {-0.0559} (-0.058)	5.487 {-0.0315} (-0.0336)
Sodium dodecylsulfate	0.0083	968.739 {-0.0912} (-0.0995)	22.407 {0.0480} (0.0397)	4.298 {0.0777} (0.0694)
Sodium decylsulfate	0.0330	860.835 {-0.0214} (-0.0544)	18.737 {0.1327} (0.0997)	3.506 {0.1688} (0.1358)
Sodium octylsulfate	0.1330	752.695 {0.0577} (-0.0753)	15.067 {0.2359} (0.1029)	2.713 {0.2835} (0.1505)
SD[f] r^2		0.103 0.77	0.075 0.79	0.097 0.80
Sodium octanoate	0.4000	609.929 {0.1820} (0.2180)	13.232 {0.2974} (-0.1026)	2.562 {0.3091} (-0.0909)
Sodium nonanoate	0.2100	667.713 {0.1285} (-0.0815)	16.419 {0.1952} (-0.0148)	3.030 {0.2341} (0.0241)
Sodium decanoate	0.1090	721.698 {0.0826} (-0.0264)	18.254 {0.1451} (0.0361)	3.426 {0.1791} (0.0701)
Sodium dodecanoate	0.0278	828.746 {0.0009} (-0.0269)	21.924 {0.0583} 0.0861 (0.0305)	4.218 0.0861 (0.0583)
SD r^2		0.088 0.91	0.046 0.98	0.061 0.94

[a] Experimental *cmc* taken from Ref. 16, [b] calculated using this Eq. [*cac*] = 3.97-1.36 logTVO, [c] Δ= *cmc* (calculated,) – *cmc* (experimental), [d] calculated using this Eq. [*cac*] = 1.52-1.09 log PT, [e] calculated using this Eq. [*cac*] = 0.730-1.03 logLPT, [f] Standard deviation.

Conclusions

On the basis of our results, one could conclude that there are good models which are statistically significant have been developed for estimating the cac of hydrotropes. In addition, the obtained results have supported the recent reports of Hatzopoulos et al. [5, 6] reflecting that all hydrotropes could act as a surfactant. It is not possible to apply a unique model for all kinds of hydrotropes and surfactants due to the change in the head group interactions in addition to gegen-ions effect. The results suggest that the estimation of cac or cmc for amphiphilic molecules using computational chemistry tools is quite possible. Finally, theoretical calculations based on density functional theory can be considered as a powerful tool for estimation the physical properties of amphiphilic molecules.

References

[1] Hopkins Hatzopoulos M, Eastoe J, Dowding PJ, Grillo I. Cylinder to sphere transition in reverse microemulsions: The effect of hydrotropes. Journal of Colloid and Interface Science 2013; 392: 304-310. DOI: 10.1016/j.jcis.2012.09.078.

[2] Eastoe J, Hopkins Hatzopoulos M, Dowding PJ. Action of hydrotropes and alkyl-hydrotropes. Soft Matter 2011;7:5917–5925. DOI: 10.1039/C1SM05138E.

[3] Srinivas V, Balasubramanian D. When does the switch from hydrotrope to micellar behavior occur? Langmuir1998;14:6658-6661. DOI: 10.1021/la980598c.

[4] Booth JJ, Abbott S, Shimizu S. Mechanism of hydrophobic drug solubilization by small molecule hydrotropes. Journal of Physical Chemistry B 2012;116:14915-14921. DOI: 10.1021/jp309819r.

[5] Hopkins Hatzopoulos M, Eastoe J, Dowding PJ, Rogers SE, Heenan, RK, Dyer R. Are hydrotropes distinct from surfactants. Langmuir 2011;27:12346–12353. DOI: 10.1021/la2025846.

[6] Hopkins Hatzopoulos M, Eastoe J, Dowding PJ, Grillo I, Demé B, Rogers SE, Heenan, RK, Dyer R. Effects of structure variation on solution properties of hydrotropes: phenyl versus cyclohexyl chain tips. Langmuir 2012;28:9332–9340. DOI: 10.1021/la301222m.

[7] Huibers PDT. Quantum-chemical calculations of the charge distribution in ionic surfactants. Langmuir 1999;15:7546-7550. DOI: 10.1021/la9903671.

[8] Huibers PDT, Lobanov VS, Katritzky AR, Shah DO, Karelson M. Prediction of critical micelle concentration using a quantitative structure–property relationship approach. Journal of Colloid and Interface Science 1997;187:113-120. DOI: 10.1016/j.jcis.1996.4680.

[9] Jalali-Heravi M, Konouz, E. Prediction of critical micelle concentration of some anionic surfactants using multiple regression techniques:A quantitative structure-activity relationship study. Journal of Surfactants and Detergents 2000;3:47-52. DOI: 10.1007/s11743-000-0112-5.

[10] Yuan S, Cai Z, Xu G, Jiang Y. Quantitative Structure–Property Relationships of Surfactants: Critical Micelle Concentration of Anionic Surfactants. Journal of Dispersion Science and Technology 2002;23:465-472. DOI: 10.1081/DIS-120014014.

[11] Roberts DW. Application of octanol/water partition coefficient in surfactant science. A Qualitative Structure Activity Relationship for micelization of anionic surfactants. Langmuir 2002;18:345-352. DOI: 10.1021/la0108050 .

[12] Li X, Zhang G, Dong J, Zhou X, Yan X, Luo M. Estimation of critical micelle concentration of anionic surfactants with QSPR approach. Journal of Molecular Structure: THEOCHEM 2004;10:119–126. DOI: 10.1016/j.theochem.2004.08.039.

[13] Katritzky AR, Pacureanu L, Dobchev D, Karelson M. QSPR Study of Critical Micelle Concentration of Anionic Surfactants Using Computational Molecular Descriptors. Journal of Chemical Information and Modeling 2007;47:782-793. DOI: 10.1021/ci600462d.

[14] Li X, Zhang G, Dong J, Zhou X, Yan X, Luo M. Correlation of critical micelle concentration of sodium alkyl benzenesulfonate, with molecular descriptors. Wuhan University Journal of Natural Science 2006;11:409-414. DOI: 10.1007/BF02832133.

[15] Khalil RA, Zarari AA. Theoretical estimation of the critical packing parameter ofamphiphilic self-assembled aggregates. Applied Surface Science 2014;318:85-90. DOI: 10.1016/j.apsusc.2014.01.046.

[16] Lindman B. Handbook of Applied Surface and Colloid Chemistry, Holmberg K, Shah DO, Schwuger MO. Editors, vol. 1. New York: John Wiley & Sons;2002. ISBN: 978-0-471-49083-8.

[17] Mills I, Cvitas T, Homann K, Kallay N, Kuchitsu K. Quantities, Units and Symbols in Physical Chemistry.2nd ed.; UK: Blackwell Science; 1993. ISBN: 0-632-03583-8.

[18] Laidler KJ, Meiser JH, Sanctuary BC. Physical Chemistry, 4th ed.; USA: Houghton Mifflin Company; 2003. ISBN: 978-0-618-12341-4.

[19] Khalil RA. A new approach to micellization parameters using iterative mathematical method. Colloids and Surface A 2006;286:51-56. DOI: 10.1016/j.colsurfa.2006.02.063.

[20] Berezin IV, Martine K, Yatsimirskii AK. Physicochemical foundations of micellar catalysis. Russian Chemical Review.1973;42:787-802. DOI: 10.1070/RC1973v042n10ABEH002744